frontiers | Frontiers in Marine Science

TYPE Original Research
PUBLISHED 20 October 2022
DOI 10.3389/fmars.2022.877616

OPEN ACCESS

EDITED BY
Erik Cordes,
Temple University, United States

REVIEWED BY
Laurence Helene De Clippele,
University of Edinburgh,
United Kingdom
Andrea M. Quattrini,
Smithsonian National Museum of
Natural History (SI), United States

*CORRESPONDENCE
Leonardo Tamborrino
ltamborrino@marum.de

SPECIALTY SECTION
This article was submitted to
Deep-Sea Environments and Ecology,
a section of the journal
Frontiers in Marine Science

RECEIVED 16 February 2022
ACCEPTED 26 September 2022
PUBLISHED 20 October 2022

CITATION
Tamborrino L, Titschack J,
Wienberg C, Purkis S, Eberli GP and
Hebbeln D (2022) Spatial distribution
and morphometry of the Namibian
coral mounds controlled by the
hydrodynamic regime and
outer-shelf topography.
Front. Mar. Sci. 9:877616.
doi: 10.3389/fmars.2022.877616

Spatial distribution and morphometry of the Namibian coral mounds controlled by the hydrodynamic regime and outer-shelf topography

Leonardo Tamborrino[1,2*], Jürgen Titschack[1,3], Claudia Wienberg[1], Sam Purkis[4], Gregor P. Eberli[4] and Dierk Hebbeln[1]

[1]MARUM – Center for Marine Environmental Sciences, University of Bremen, Bremen, Germany, [2]Green Rebel, Crosshaven, Ireland, [3]Senckenberg am Meer, Marine Research Department, Wilhelmshaven, Germany, [4]Department of Marine Geosciences, CSL- Center for Carbonate Research, University of Miami, Miami, FL, United States

Cold-water corals mounds develop over millennial timescales as a result of sustained coral growth and concurrent with sediment deposition within their coral frameworks. So far, coral mounds have been primarily investigated as deep-sea biodiversity hotspots and geo-biological paleo-archives, whereas their morphological appearance and spatial arrangement have received much less attention. Here, we analysed the spatial distribution and the morphometry of coral mounds that developed on the Namibian shelf during a single short period dating back to the Early. The spatial distribution of these "early-stage" mounds and their morphological characteristics revealed a hierarchy of three different patterns. These comprise an alongslope mound distribution at a regional scale (*first-order* pattern), a topography-steered downslope alignment of mounds at a local scale (*second-order* pattern), and a hydrodynamic-controlled downslope orientation of the individual mounds at a mound scale (*third-order* pattern). In addition, because the Namibian mounds rarely exceed 20 m in height, key steps in the development of early-stage coral mounds (e.g. elongation, merging, limited gain in height compared to lateral extension) have been identified. With increasing size, coral mounds are more elongated, parallel to the prevailing tidal system, which is interpreted to reflect the transition from an "inherited" to a "developed" mound morphology. Besides supporting this earlier hypothesis on mound development, we could show that this transition takes place when the Namibian coral mounds reach ~150 m in length and ~8 m in height. This study reveals that the spatial-morphological appearance of coral mounds, often treated as a descriptive information, can provide valid information to understand their formation.

KEYWORDS

cold-water corals, coral mound formation, morphometry, internal tides/waves, underlying topography, spatial analysis

Introduction

Coral mounds are seafloor structures built by framework-forming scleractinian cold-water corals (CWC; Roberts et al., 2006). The development of the coral mounds firstly depends on CWC proliferation, controlled by a wide range of environmental parameters (dissolved oxygen concentrations, temperature, aragonite saturation state, pH, etc.; e.g., Davies et al., 2008). When their physic-chemical boundary conditions are met, the distribution of CWC is strongly controlled by food supply, since CWC are sessile opportunistic suspension feeders with a diet based on particulate and dissolved organic matter (Kiriakoulakis et al., 2005; Duineveld et al., 2007; Dodds et al., 2009; Mueller et al., 2014). The required food is mostly delivered by a moderate to strong hydrodynamic regime induced by geostrophic bottom currents and/or turbulent mixing triggered by internal waves, downwelling, cascading density currents, and Taylor columns (e.g., Frederiksen et al., 1992; Taviani et al., 2005; White et al., 2005; Thiem et al., 2006; Mienis et al., 2007; Davies et al., 2009; Mienis et al., 2009; Mienis et al., 2012; van Haren et al., 2014). The bottom currents do not only deliver food to the CWC, but also suspended sediments, which become trapped (baffling effect) by the coral frameworks (Mienis et al., 2019; Bartzke et al., 2021; Hennige et al., 2021). This baffled sediments within the coral frameworks usually contributes >50% to the coral mound deposits (e.g., Dorschel et al., 2007; Titschack et al., 2015; Wang et al., 2021).

Coral mounds are often clustered in coral mound provinces (CMPs) with 10s to 1000s of mounds (e.g., Wheeler et al., 2011; Lo Iacono et al., 2014; Glogowski et al., 2015; Hebbeln et al., 2019; Mareano, 2020; Steinmann et al., 2020). Most of these CMPs occur around the continental margins of the Atlantic Ocean, on the upper to mid continental slopes (e.g., Kenyon et al., 2003; Colman et al., 2005; Grasmueck et al., 2006; Le Guilloux et al., 2009; Carranza et al., 2012; Hebbeln et al., 2014; Glogowski et al., 2015; Steinmann et al., 2020), but a large number of mounds appear also on continental shelves (e.g., Reed, 2002; Fosså et al., 2005; Douarin et al., 2013; Tamborrino et al., 2019). Often the occurrence of the CMPs correspond to present or past boundaries of intermediate water masses (Dullo et al., 2008; White and Dorschel, 2010; Mohn et al., 2014; Matos et al., 2017; Wang et al., 2019). Density gradients (pycnocline) between water-mass boundaries allow for the accumulation of (re-)suspended organic particles and fine-grained sediments, resulting in the formation of intermediate and/or bottom nepheloid layers (Wang et al., 2001; Cacchione et al., 2002; Hosegood et al., 2004; Cheriton et al., 2014). Density gradients also play a key role for the formation of internal waves when intersecting relative steep slopes, which causes turbulent mixing (Garrett and Kunze, 2007; Klymak et al., 2011; Pomar et al., 2012; van Haren and Gostiaux, 2012). Both processes support CWC proliferation and coral mound formation as they enhance the availability and supply of food and sediments (Frederiksen et al., 1992; Mienis et al., 2007; Davies et al., 2009; White and Dorschel, 2010; Hebbeln et al., 2014; Wang et al., 2019).

The presence of a suitable hard substrate of any size (from rocky outcrop to mm-sized bioclasts or gravel) represents an important prerequisite for the settlement of CWC planula (Wilson, 1979). Moderately enhanced hydrodynamics increasing the probability of food capture by the CWC is another advantageous prerequisite (Wheeler et al., 2007). This leads to a preferential CWC settlement on pre-existing seabed topography of variable scale, such as erosional features (De Mol et al., 2005), mud volcanoes (Wienberg et al., 2009; Margreth et al., 2011), underlying faults (Haberkern, 2017), iceberg plough marks (Freiwald et al., 1999; Fosså et al., 2005) and dropstones-boulders (Hübscher et al., 2010; Hebbeln et al., 2012; Savini et al., 2014; Buhl-Mortensen et al., 2017), which eventually reflect preferred sites for the initiation of coral mounds. The underlying topography often conditions the spatial distribution, but also the morphology of mounds in their early-stage development (defined as "inherited" mound morphology; see Wheeler et al., 2007), with such mounds largely reflecting the morphology of the underlying topographic features. As CWCs continue to grow, mound height and volume increase, and the mounds become increasingly subject to the local hydrodynamic regime. The inherited mound morphology transforms into a "developed" morphology, meaning the underlying topography becomes increasingly attenuated and the mound assumes its own morphology, which reflects rather its interaction with the prevailing hydrodynamic conditions (Wheeler et al., 2007). Coral mound morphologies, detected by multibeam echosounders (MBES), side-scan sonar and seismic reflection data, exhibit a wide qualitatively-described morphological variety: simple conical, conical with an oval footprint, elongated, arcuate, ridge-like, V-shaped and multi-peaked (e.g., Colman et al., 2005; Grasmueck et al., 2006; Wheeler et al., 2007; De Haas et al., 2009; Hebbeln, 2019), but discrete quantitative measurements are still rare (Mortensen et al., 2001; Huvenne et al., 2003; Correa et al., 2012b; Lim et al., 2018). To document the transition from inherited to developed morphologies or other controls on mound distribution/formation in CMPs, a large-scale spatial and morphometric analyses are needed but are still largely lacking.

Coral mounds can rise from their surrounding seafloor from a few meters (e.g., Foubert et al., 2008; Somoza et al., 2014; Collart et al., 2018; Lim et al., 2018) up to >350 m (Kenyon et al., 1998) and have a lateral extension that can reach the km-size scale (e.g., Beyer et al., 2003; Colman et al., 2005; Mienis et al., 2007). Most of the morphometric information on coral mounds is based on manual measurements describing mostly the size ranges or the highest values (e.g., Colman et al., 2005; Wheeler et al., 2007; De Haas et al., 2009; Angeletti et al., 2020; Steinmann et al., 2020). Crucial for morphometric analysis of coral mounds are objective measurements based on solid definitions. Already

basic terrain variables obtained from the digital elevation model (DEM), such as slope angle or bathymetric positioning index, allowed (semi)automated identification and extraction of the coral mounds by thresholding and the subsequent determination of morphometric parameters like footprint area and lateral extension (Correa et al., 2012b; Hebbeln et al., 2019). However, a relevant morphometric parameter, such as mound height, has often been measured only manually (Huvenne et al., 2003; Lo Iacono et al., 2014; Vandorpe et al., 2017; Hebbeln et al., 2019).

In recent years, a large variety of mapping classification methods for coral mounds based on manual, semi-automated, automated and machine-learning-based approaches have been developed (Lim et al., 2021). These methodologies benefited from high-resolution MBES datasets (e.g., De Clippele et al., 2017a; Lim et al., 2018), combined with imagery data (side-scan sonar, ROV photogrammetry; e.g., Savini et al., 2014; Price et al., 2019). Often the focus of these spatial-mapping investigations was rather on ecological aspects of CWC colonies and their associated fauna (e.g., Boolukos et al., 2019; Corbera et al., 2019; De Clippele et al., 2021) than on coral mounds as morphological features. The morphology of coral mounds represents a synthesis of complex biological and physical processes interacting on geological timescales, which likely can be assessed retrospectively by the extraction of morphometric parameters. Some morphometric parameters, such as mound height and length, are commonly mentioned for coral mounds (e.g., De Mol et al., 2002; Colman et al., 2005; Foubert et al., 2005; Mienis et al., 2006; De Mol et al., 2007; Carranza et al., 2012; Hebbeln et al., 2014; Angeletti et al., 2020), but only few studies used these information to classify coral mounds (e.g., Mortensen et al., 2001; Lo Iacono et al., 2014; Vandorpe et al., 2017; Lim et al., 2018) and even less linked mound morphology with mound formation processes (Correa et al., 2012a; Hebbeln et al., 2019).

Our study presents a detailed analyses of the spatial distribution pattern and morphometric parameters of coral mounds, which were recently discovered on the outer Namibian shelf (Hebbeln et al., 2017). The large number of >2000 small mounds forming the Namibian CMP (Tamborrino et al., 2019) provides an excellent and extensive database to explore the potential of spatial-morphometric analyses to better understand the effect of regional oceanographic and local hydrodynamic processes and the underlying topography on mound formation. Due to extremely low ambient dissolved oxygen concentrations nowadays, no living corals occur on these mounds (Hanz et al., 2019). According to Tamborrino et al. (2019), the Namibian coral mounds show the typical mound composition of coral fragments embedded in a matrix of hemipelagic sediments and formed during a well-defined short period during the Early to Mid-Holocene, which suggest well-constrained environmental conditions during their development. Accordingly, by analyzing the spatial distribution and morphology of the Namibian coral mounds, this study reveals a hierarchy of three different (first- to third-order) patterns controlled by partly competing influence of the regional oceanography, local hydrodynamics and underlying topographic features. Finally, our study outlines an approach to exploit spatial and morphometric analyses that could be easily applied to other CMPs, which would allow an observer-independent comparison of different CMPs and could contribute to the understanding of basic principles of coral mound development.

Material and methods

Study area

The Namibian CMP consists of ~2,000 coral mounds in ~160-270 m below sea level (mbsl) extending over a distance of (at least) 80 km along the northern outer Namibian shelf/upper slope (Figure 1). The Namibian coral mounds are grouped in three clusters or sub-provinces, which occur on top (Escarpment mounds) and west (Squid Mounds, SQM; Coral Belt Mounds, CBM) of a large NNE-SSW-trending Escarpment (Tamborrino et al., 2019). The Namibian mounds developed during one short (~5 kyr) period corresponding to the Early to Mid-Holocene. Today, they are densely covered by fossil coral rubble clogged by hemipelagic sediments (Tamborrino et al., 2019).

The water masses along the Namibian margin are surface waters (0-85 mbsl) and the central water masses (85-480 mbsl), South Atlantic Central Water (SACW) and Eastern South Atlantic Central Waters (ESACW). Southern-sourced surface waters and the ESACW are carried equatorward from the southern tip of Africa (37°S) by the Benguela Current, while the oxygen-depleted SACW and related surface waters are transported southward from the Angolan margin by the Angola Current (AC) and the Poleward Undercurrent (PUC; Figure 1A). The two surface water masses converge at the Angola-Benguela Front (14-17°S, ABF), which is a pronounced frontal system (von Bodungen et al., 2008). Within the underlying central water masses, no sharp boundary exists between the SACW and ESACW, but rather a broad transition zone (Mohrholz et al., 2008). The southward migration of the SACW by the PUC contributes to the well-developed OMZ off Namibia (Schmidt and Eggert, 2016). Here, the OMZ is further influenced by the Benguela Upwelling System (BUS), which enhances surface productivity leading to an increased export of organic matter and enhanced oxygen consumption (Schmidt and Eggert, 2016). The Namibian coral mounds are today located within the core of the OMZ (160-270 mbsl), where dissolved oxygen concentrations are below 0.5 ml l-1 and even drop to 0.1 ml l-1 (Hanz et al., 2019). An intensification of the

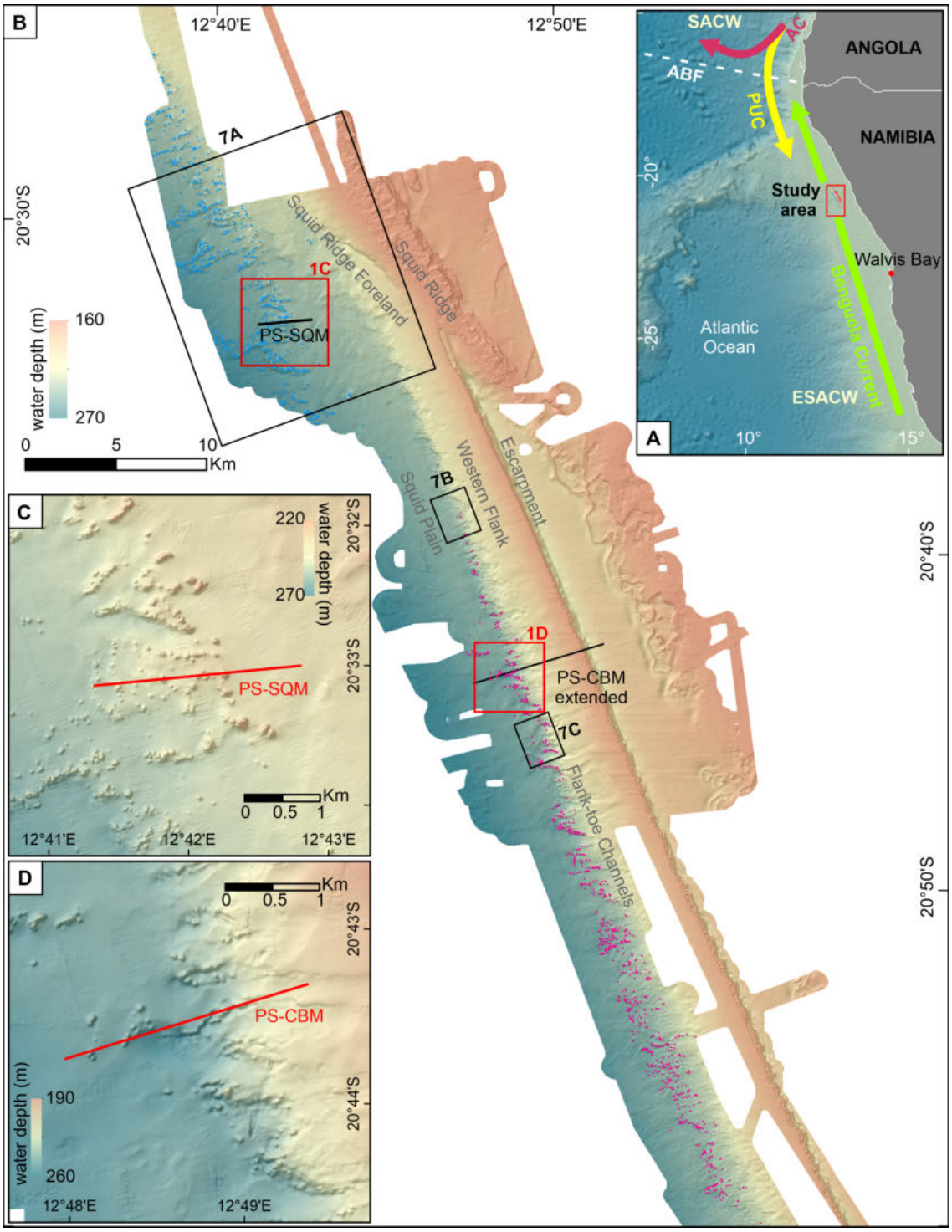

FIGURE 1
(A) Overview map showing the oceanographic circulation along the Namibian coast. Red square highlights the study area. Bathymetric map **(B)** showing the Namibian coral mound province. Dots are indicative of the mound peaks, light blue for Squid Mounds (SQM) and pink for Coral Belt Mounds (CBM). For the position of the Escarpment Mounds see Tamborrino et al. (2019). **(C, D)** Detailed view of some SQM and CBM, respectively. Position of the Parasound profiles (see Figure 3) are shown by black (panel B) and red lines (panels **C, D**). Black boxes indicate the position of the 3D view maps in Figure 7. Acronyms: ABF-Angola Benguela Front; AC-Angola Current; PUC-Poleward Undercurrent; SACW-South Atlantic Central Waters; ESACW-Eastern South Atlantic Central Waters. PS-Parasound profiles.

BUS, and therefore, of the OMZ likely caused the Mid-Holocene demise of the CWC off Namibia (Tamborrino et al., 2019).

At a regional scale, large portions of organic particles, derived from the BUS, are laterally transported and deposited on the Namibian outer shelf, contributing to the formation of intermediate nepheloid layers (INL, Giraudeau et al., 2000; Inthorn et al., 2006). A semi-diurnal internal tide has been measured by a benthic lander also in the Namibian CMP, close to the CBM (Hanz et al., 2019). Thus the formation of this INL is likely derived from the interaction between topography of the outer Namibian shelf and the pycnocline, with the formation of the internal tide at the boundary between PUC-delivered SACW and the surface waters, that keep particles in suspension (Zabel et al., 2019).

Hydroacoustics

The hydroacoustic data for this study were collected during *R/V Meteor* expedition M122 (Hebbeln et al., 2017) and during *R/V Maria S. Merian* expedition MSM 20-1 (Geissler et al., 2013). Seabed mapping was performed by two different hull-mounted Kongsberg multibeam echosounders (MBES): EM710 (70-100 kHz) and EM1002 (95 kHz) during expedition M122 and MSM20/1, respectively. The EM710 acquired 200 beams per ping and 400 soundings ("soft-beams") in the high-density mode covering a depth range of several meters up to ~800 m The EM1002 emitted 111 beams per ping, covering a depth range of 2-1000 m. During both cruises, the spatial integrity of the mapping data was achieved by combining the ship's inertial navigation systems including differential global positioning system information with motion data (roll, pitch, heave) provided by the motion reference units (Kongsberg Seapath 320 and 200, respectively for *R/V Meteor* and *R/V Maria S. Merian*). Based on comparing the two independent MBES bathymetric data sets, their vertical precision is ±50 cm. For the correction of the hydroacoustic measurements, sound velocity profiles through the water column were repeatedly recorded using either a CTD or sound velocity probes. The open-source software package MB-System v.5.3.1 (Caress and Chayes, 1995) was used for bathymetric data post-processing, editing and evaluation. MBES data were interpolated to make a digital elevation model (DEM) with 10 x 10 m grid cell size (using MB-system mbgrid tool). Maps were produced with ESRI ArcGIS v.10 and Global Mapper v.20.

During the M122 expedition, seismoacoustic sub-seafloor information was acquired with ATLAS PARASOUND PS70, a deep-sea sub-bottom profiler that utilizes the parametric effect based on non-linear relation of pressure and density during sonar propagation. The sub-bottom profiling relies on the signal from the secondary low frequency at ~4 kHz. The opening angle of the transducer array is 4° by 5°, which corresponds to a footprint size of about 7% of the water depth. The data acquisition was performed with the real-time values of surface sound velocity measured close to the Tx/Rx-array (System C-Keel) and a static sound velocity profile of 1500 m s^{-1} (C-Mean). The program Teledyne PARASTORE 3.0 was used for storing and displaying echograms. Within the Teledyne Hydromap Control program, the proper hydroacoustic settings were set before the acquisition. Kingdom IHS was used for reproducing the PARASOUND profiles with a bandpass filter (low-high cut 2000-4000 Hz, low-high pass 2500-4500 Hz).

Mound extraction and morphometric analyses

Analyses of morphometric data were carried out for each mound following the workflows presented by Purkis et al. (2007). Most of the processing was performed with the Petrel™ software package (Schlumberger, license: University of Miami, US). The coral mound base was defined following the methodological approach of Correa et al. (2012b) using the dip angle map ("Petrel/Op./Surface operations/Dip Angle"), generated from the original DEM, to extract closed polygons describing the mound footprints that follow the 3°-contour line ("Petrel/Op./Convert points, polygons, surfaces/Create intersection with plane"). This 3°-cutoff has been qualitatively validated with a comparison between the DEM and the dip angle (Figure 2). Small-scaled polygons obtained by the automated 3° cut-off value (e.g. bathymetry artifacts or decrease in slope within mound perimeter) were removed. Unrealistic mound footprint polygons, more common by CBM due to steeper underlying slope, were corrected by removing single polygon nodes. Polygon nodes were also manually edited to split twin-peaks mounds on the base of higher cut-off dip angle values (5°). The DEM was subsequently re-gridded to generate hypothetical bathymetric maps without mounds ("Petrel/Calc./Eliminate inside" to remove the coral mounds, and "Utilities/Make-edit new surface" to create an interpolated map from the DEM with no mounds), for which the vertical relief beneath each removed mound was interpolated from the mound perimeters. The newly interpolated surfaces were then subtracted from the original DEMs to calculate the volume and heights of the coral mounds. Only features with a footprint area greater than 900 m^2 (corresponding to a two-dimensional array of 3 × 3 DEM grid cells) and with a height of >2 m above the surrounding seafloor (4 × 0.5 m of vertical precision) were considered as coral mounds. Because the small size (mostly <2 m height) and number (138) of the Escarpment mounds (Tamborrino et al., 2019), the analyses reported here focus on the CBM and SQM only (Figure 1).

A summary of the morphometric parameters used to quantify the spatial variability of the Namibian coral mounds is presented in Table 1. For all obtained morphometric parameters descriptive statistics, such as mean, standard

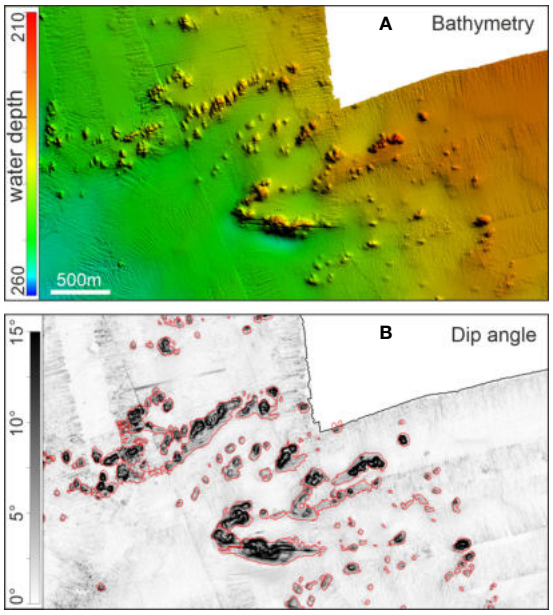

FIGURE 2
Comparison between **(A)** digital elevation model (DEM) and **(B)** dip angles exemplified for an area within Squid Mound cluster. The red line indicates the polygons obtained by applying the 3°-cutoff value, after editing. DEM and dip angles are gridded at 10 m. The scale (shown in the DEM frame) bar is equal for both frames. This highlights also the morphological appearance of merging coral mounds.

deviation (SD) and median, were determined. To evaluate the spatial distribution and density of the coral mounds, heatmaps were calculated with the kernel density tool of ArcGIS 10.3 and an output raster cell neighborhood of 50 m and a search radius of 1 km, after projecting the DEM into UTM Zone 33S, following Lim et al. (2018). Slope and aspect maps are based on the interpolated DEM without coral mounds (grid size: 20 m) and were calculated with the ArcGIS tool Benthic Terrain Modeler, using the Horn method (Horn, 1981).

To differentiate between inherited and developed mound morphologies (*sensu stricto* Wheeler et al., 2007) we evaluated the morphometric analysis of the coral mounds (i.e, orientation, size parameters) in relation to their size (relative to their height and PAX length) and compared it with hydrological data (i.e., current directions) obtained by benthic lander to characterize the local hydrodynamic regime (Hanz et al., 2019). Inherited coral mounds should generally be marked by no preferred orientation and low degree of elongation, while developed coral mounds should be elongated and exhibit a clear preferential orientation in line with the prevailing hydrodynamic regime. Additionally, we extracted geomorphometric parameters of the underlying topography (slope, aspect) to assess its potential additional influence on the coral mound morphology.

Results

Prominent morphological features of the Namibian coral mound province

The MBES bathymetric map of the Namibian CMP covers an area of 1179 km2 along the northern Namibian shelf (Figure 1). The most prominent morphological feature is represented by a straight ~63-km-long NNW-SSE trending Escarpment with heights of up to ~50 m (top of the Escarpment: ~165 mbsl). Its eastern steep margin exhibits a slope angle of up to 40° and ends in a moat (maximal depth: ~215 mbsl) developed parallel to the Escarpment. Several irregular-shaped erosive features occur east of the Escarpment (~150-190 mbsl; Figure 1B). The Western Flank of the Escarpment (~ 165-220 mbsl) is gently dipping (slope angle <5°) and shows no pronounced surface features. Close to its western limit just below 220 mbsl, slope-indenting channels and headwalls (referred to as Flank-toe Channels, 220-260 mbsl, Figures 1B, D) incise the foot of the Western Flank. Most of these channels have a NE-SW orientation, hence are orientated perpendicular to the shelf. The area west of the Flank-toe Channels changes towards the gently westward-dipping Squid Plain (240-310 mbsl; Figure 1B). The northern termination of the Escarpment (at ~20°34'S) is bordered by the NW-SE-trending Squid Ridge (top: 140 mbsl). The western flank of the Squid Ridge is shaped by a 5-km-long headwall (up to 20 m high). West of this headwall, the Western Flank of the Escarpment fades into a slightly westward-dipping slope with a faintly-carved surface (referred to as Squid Ridge Foreland, 210-240 mbsl). West of the Squid Ridge Foreland, low relief furrows incise the flat morphology of the Squid Plain.

The PARASOUND profiles exhibit a relatively good penetration (>50 m) and reveal mainly seaward-dipping reflectors (Figure 3). Only close to the Flank-toe Channels the sub-bottom reflectors are partly horizontal (Figures 3B, C). Furthermore, some unconformities can be observed beneath the seabed, with the seabed itself also partly representing an erosive surface (Figures 3A–C). PARASOUND profiles do not show any buried portions of the SQM and the CBM, which are sitting on topographic highs made up of exposed older strata (Figure 3).

Spatial distribution and density pattern of the Namibian coral mounds

A total of 659 and 542 coral mounds were extracted from the SQM and CBM sub-provinces, respectively. These numbers are slightly lower as initially proposed by Tamborrino et al. (2019; SQM: 959; CBM: 896), who manually counted the total number of mound peaks. This difference is ascribed to the here applied cutoff-

TABLE 1 Summary of parameters used to quantify the spatial-morphometric variability of Squid (SQM) and Coral Belt Mounds (CBM) off Namibia.

Parameter	Definition	Unit	Range	
			SQM	CBM
Mean depth	Average depth within the mound perimeter	mbsl	211 – 266	225 – 258
Mound footprint area	Area of mound perimeter based on 3° cutoff	m^2	900* – 115,639	900* – 47,040
Mound height	Maximum elevation within mound perimeter, after subtracting the interpolated surface without mounds	m	2* – 21	2* – 15
Mound volume	Volume of the mound above the interpolated surface without mounds	m^3	92 – 492,198	270 – 114,282
PAX (principal axis) length	Length of the principal axis crossing the centroid of the mound footprint (Peura and Iivarinen, 1997)	m	38 – 1,100	39 – 428
OPAX length	Length of the axis orthogonal to PAX	m	4 – 255	9 –205
PAX direction	Direction of the principal axis		1 – 180	0 – 180
PAR	OPAX/PAX ratio	0 to 1 ratio	0.03 – 0.97	0.06 – 0.98
Average slope	Average slope angle within the mound perimeter		2 – 14	2 – 24
Underlying-mound average slope	Average slope angle within the mound perimeter on the interpolated surface after mound removal		0 – 8	1 – 12

*defined lower threshold for mound detection.

based method to separate multi-peak mounds and the exclusion of very small mounds (height: <2 m, footprint: <900 m^2).

The SQM extend for at least 5 km downslope and 20 km alongslope on the northern portion of Squid Plain (Figure 1B), where they partly sit on the margin of low-relief furrows (Figure 1C). Further to the south, the CBM are mostly associated with the Flank-toe Channels (Figures 1B, D) and stretch in a narrow (mostly <3 km) belt for >40 km from SSE to NNW. Together the SQM and the CBM encompass ~1,200 mounds that are located between ~210 and 270 mbsl (Figure 4). The 659 SQM cover a slightly broader depth interval (~210-270 m) with a slightly deeper mode of 250-255 mbsl compared to the 542 CBM occurring between ~220-260 mbsl with a mode of 240-245 mbsl (Figure 4).

The extension of the mapped portion of the two sub-provinces is given by the heatmaps (based on outer limits of all 1 km radii around the individual mound peaks), which amount to ~95 km^2 for the SQM and ~100 km^2 for the CBM. Although in both areas mound densities vary between 1 and 40 mounds/km^2 (Figures 5A, D), the average density is slightly higher for the SQM (10.1 mounds/km^2) compared to the CBM (8.9 mounds/km^2). The sum of the mound footprint areas covers 6.0 % and 2.9 % of the extension of the SQM and CBM sub-provinces, respectively. The heatmaps highlight a general alongslope distribution of the coral mounds in both sub-provinces. In detail, areas of high concentrations of SQM stretch in different directions such as NE-SW, E-W and NW-SE (Figure 5A). The CBM are largely concentrated in a general belt-like NW-SE trend (Figure 5D).

The seabed area occupied by the Namibian coral mounds is relatively flat with a mean slope of 0.7° (SD 0.7°) in the SQM area and a slightly steeper mean slope of 1.5° (SD 1.5°) in the CBM area (Figures 5B, E). This slight difference is also expressed by more topographic features characterizing the CBM (channels indenting the flank-toe) than the SQM area. The Namibian CMP covers a seabed area with a general SW orientation, with the topography underlying the SQM sub-province trending more towards the S, while the aspect of the CBM sub-province is more directed to the west (Figures 5C, F). Areas of slightly-dipping E-orientated values appear on the eastern shallow limit of the SQM (Figure 5C), as also indicated by the slope change in the PARASOUND profile (Figure 3A).

Morphometric parameters of the Namibian coral mounds

Size-related morphometric parameters, such as footprint area, volume, height and PAX (principal axis of the mound footprint polygon) length, show similar trends in both sub-provinces, the SQM and the CBM (Figures 6A–D). The exponential decline of mound numbers with increasing size indicate the dominance of small mounds off Namibia: most of the SQM and CBM have a footprint area of <10,000 m^2 (SQM: 78%, CBM: 90%), a volume of <10,000 m^3 (SQM: 70%, CBM: 79%), a height of <10 m (SQM: 88%, CBM: 98%), and a PAX length of <120 m (SQM: 67%, CBM: 78%). Despite similar sizes of most coral mounds, differences between the SQM and CBM are highlighted by comparing the maximum (Table 1) and mean values (Figure 6). The mean values represent the overall similarity of the two sub-provinces with slightly higher average values for the SQM (Figure 6), While the

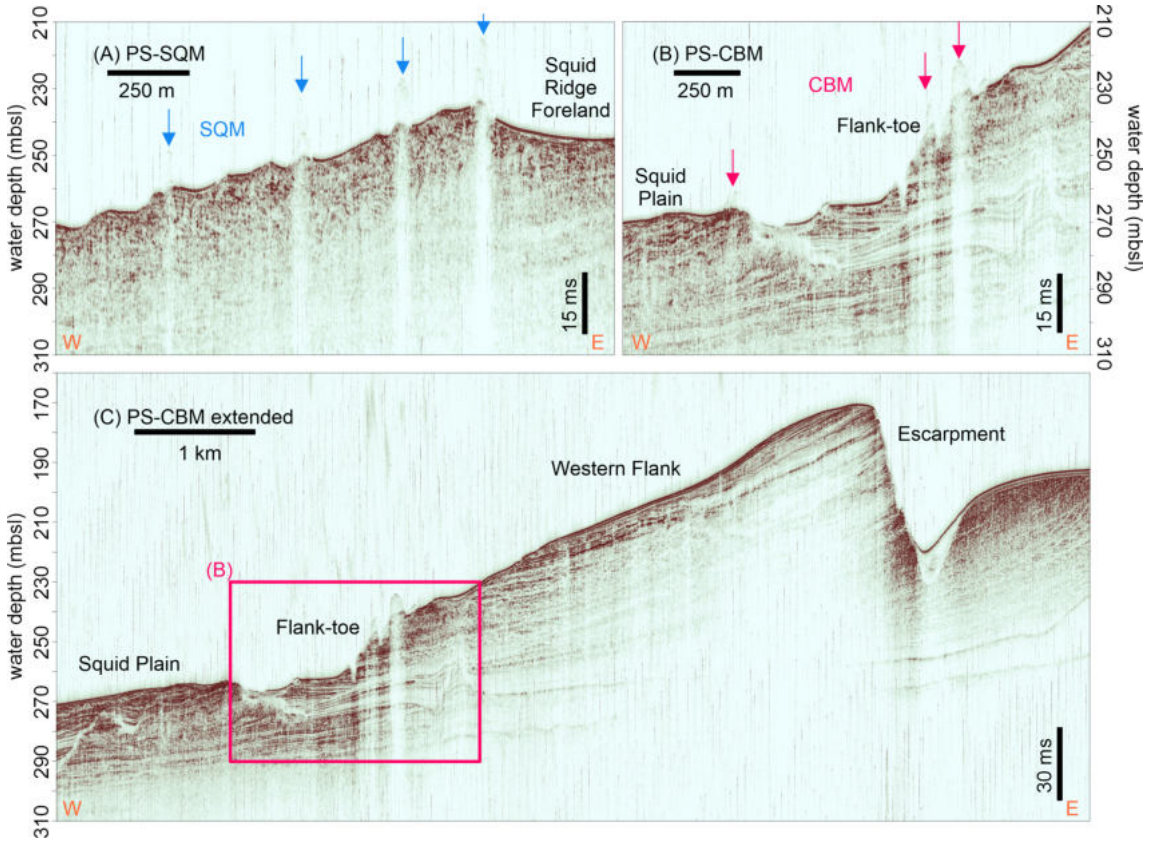

FIGURE 3
PARASOUND sub-bottom profiles crossing the major topographical features of the Namibian coral mound province: **(A)** the Squid Mounds (SQM), **(B, C)** the Coral Belt Mounds (CBM). Position of the PARASOUND profiles is shown in Figure 1. Orientation (E-W) is indicated at the bottom of the profile (orange letters).

major differences are caused by the presence of a few relatively large mounds among the SQM (Table 1; Figure 6).

The shape-related parameters reveal some more differences between the two sub-provinces. The principal axes ratio (PAR) shows mostly similar trends in the two sub-provinces (Figure 6E). However, a larger number of the SQM (21%) show a PAR of <0.3, indicative of more elongated mounds on the Squid Plain compared to the CBM (16%). The PAX directions of the SQM have three maxima: 45°, 90-95° and 135°, while the PAX directions of CBM are generally concentrated between 55° and 100° (Figure 6F). The average slopes of the mounds show a similar distribution for both the SQM and CBM (Figure 6G). However, the SQM have a much steeper mean slope angle than the CBM, considering the number of mounds with slope angles of <6° (SQM: 25%, CBM: 40%) and >8° (SQM: 40%, CBM: 27%). The average slope of the underlying topography where the coral mounds sit on, have very small values of <3° for 79% of the SQM and for 58% of the CBM (Figure 6H). However, values steeper than 8° occur only on CBM, although in rather low numbers (2%, Figure 6H).

Discussion

Spatial distribution

The Namibian coral mounds occur on the outer shelf in relatively shallow water depths (210 – 270 mbsl, Figure 4) compared to the majority of CMPs in the Atlantic Ocean that are found on the upper continental slope in much deeper depths of 500 and 1,000 m (e.g., Schroeder, 2002; Wheeler et al., 2007; Hebbeln et al., 2019; Galvez, 2020; Raddatz et al., 2020; Steinmann et al., 2020). *Lophelia*-(Purkis et al. 2007) dominated mounds developed in shallow shelf waters are mainly known from high latitudes in the NE Atlantic, such as off Norway (38 - 400 mbsl, e.g., Mortensen et al., 2001; Fosså et al., 2005; Lindberg et al., 2007; Lavaleye et al., 2009) and off Scotland (Mingulay Reef, 90-200 mbsl, Duineveld et al., 2012), while the Namibian CMP is the first shelf site described from the SE Atlantic and positioned in low latitudes. All shelf coral mounds (Norway, Scotland, Namibia) have in common that they have relatively small elevations (<20 m; Bøe et al., 2016; De Clippele et al., 2017b), which reflects most

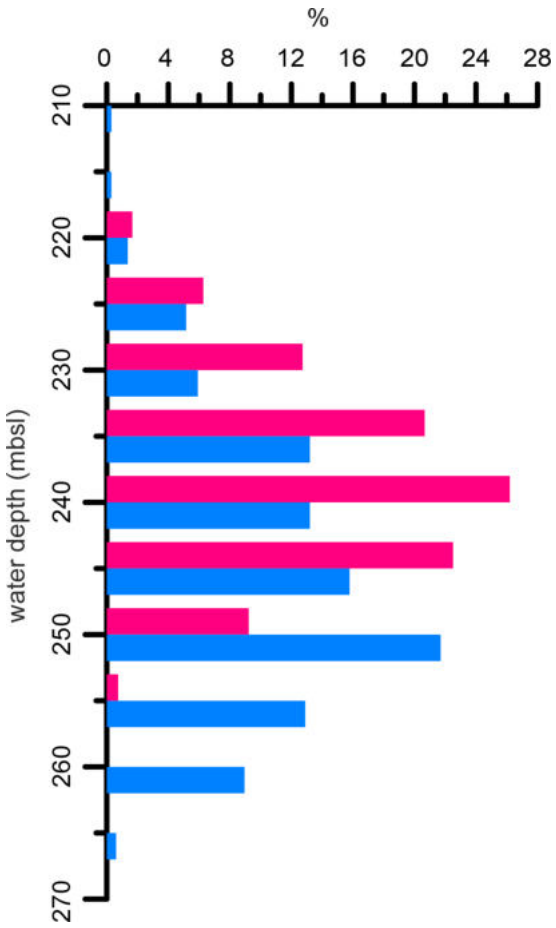

FIGURE 4
Histogram plot showing the relative depth distribution of the Squid Mounds (light blue) and Coral Belt Mounds (pink) based on the mean water depth of the mound footprint area. Interval of the bin: 5 m. Histogram bar plotted at upper limit (lowest water depth).

likely their short (but often rapid) formation history that started only during the Early Holocene with the drowning of the shelves during the deglacial sea-level rise (López Correa et al., 2012; Douarin et al., 2013; Tamborrino et al., 2019).

The Namibian coral mounds extend alongslope for >80 km in a narrow water depth interval (<60 m) in NNW-SSE direction (Figures 1, 4, 5A). This regional-scale alongslope distribution (*first-order* pattern) is also observed in other Atlantic CMPs, e.g., on the Irish margin (De Haas et al., 2009; White and Dorschel, 2010; Wienberg et al., 2020), the southern Gulf of Mexico (Hebbeln et al., 2014), and the Argentine margin (Steinmann et al., 2020). In some CMPs, coral mounds are distributed in two alongslope chains (Porcupine Seabight, Beyer et al., 2003; Atlantic Morocco, Hebbeln et al., 2019) or are merged to more or less continuous alongslope ridges (Mauritania, Colman et al., 2005; Angola, Hebbeln et al., 2020). Considering that the development of coral mounds relies primarily on the proliferation of the CWC, which depends on environmental conditions fitting their physiological needs (e.g., food, dissolved oxygen, temperature; Roberts et al., 2009; Davies and Guinotte, 2011; Wienberg and Titschack, 2017), suggests that the regional-scale distribution of coral mounds is primarily controlled by the regional oceanography. Off Namibia, the occurrence of intermediate nepheloid layers (Inthorn et al., 2006) along the boundary between the SACW and the surface waters (Hanz et al., 2019) probably plays a key role for the food supply to the CWC and, thus, these present a potential mechanism that could have triggered the observed alongslope distribution of the Namibian coral mounds.

On a local scale the distribution density maps show a downslope component in the SQM distribution (Figure 5A). A comparable distribution pattern is not observed (on the heatmaps) for the CBM (Figure 5D), which might be explained by the steeper slope of the underlying topography causing most likely the narrower E-W extension of the CBM sub-province. However, a closer look at the MBES bathymetry reveals that the CBM have been formed along the rims of the Flank-toe Channels, comparably to the SQM that are aligned along the low-relief furrows in the Squid Plain (Figure 7). These downslope-directed topographic features have an erosive origin and were most likely formed before corals colonized the area. Elevated topographic features at the seafloor are well known as preferential settling grounds for CWC (and subsequent formation of coral mounds) due to the related enhanced turbulence that supports food (and sediment) supply (e.g., Genin et al., 1986; Frederiksen et al., 1992; White, 2003; White et al., 2005; Mienis et al., 2007; Mohn et al., 2014). Consequently, off Namibia pre-existing sea floor topography is suggested to play an important role on a local-scale and the downslope component in SQM and CBM distribution, mainly steered by this underlying topography, reflects a distinct *second-order* pattern for the spatial distribution of the coral mounds. On the individual mound scale, many Namibian coral mounds have a downslope orientation (*third-order* pattern) as reflected by their PAX angles (Figures 6F and 8). The PAX angles of the CBM show a broad range of preferred directions between 55° and 100° that overlaps with two PAX angle maxima of the SQM (at 45° and 90°), which have an additional maximum at ~130° (Figure 8). The observed range of PAX angles follows the predominantly SW-dipping regional topography (Figures 5C, F, 8) and aligns with the direction of the regional tidal currents (Hanz et al., 2019). Coral mounds with specific orientations as a response to hydrodynamic forcing are often observed (e.g., Mortensen et al., 2001; Beyer et al., 2003; Masson et al., 2003), however, depending on the overall setting, these are either aligned to the main current direction (i.e., *first-order* pattern; e.g., Wheeler et al., 2011; Mienis et al., 2014) or to internal tides (e.g., Hebbeln et al., 2019). As off Namibia orientations of the mounds are mostly parallel to the direction of the internal tides

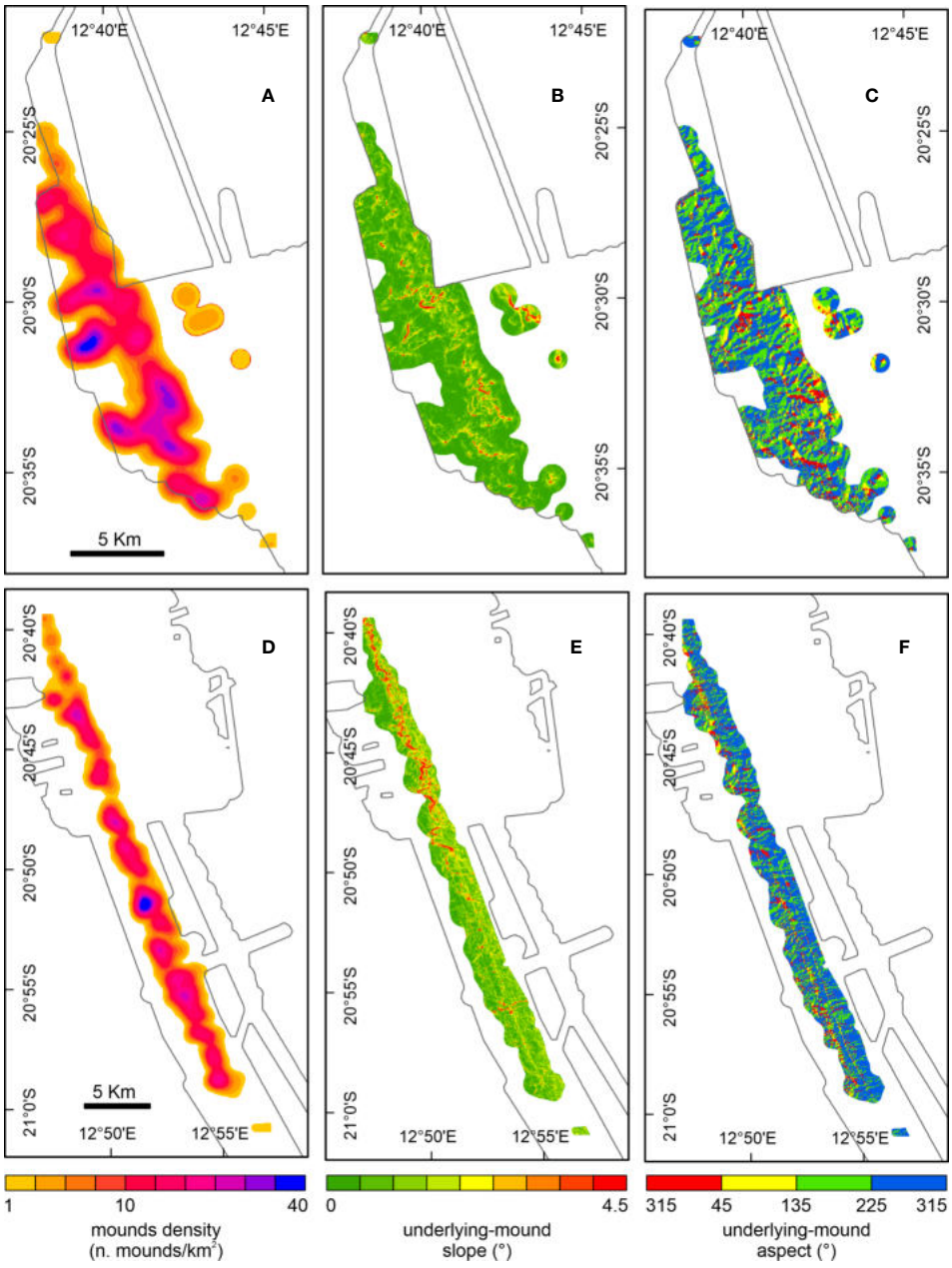

FIGURE 5
Density of coral mounds, slope and aspect maps of mound-underlying topography for Squid Mounds **(A–C)** and Coral Belt Mounds **(D–F)**. Density is expressed as a number of mound peaks per km2 over a neighborhood of 50 m retrieved from a search radius of 1 km. Zero values are excluded. Slope and aspect are computed by the ArcGIS Benthic Terrain Modeler using DEM after mound removal. In the background, the border of the bathymetric dataset is indicated by a thin black line (see Figure 1 for orientation).

(and perpendicular to the main current direction), thus, tidal action appears to be the dominant forcing causing the elongation of the mounds and the *third-order* pattern.

In summary, the spatial distribution and the orientation of the Namibian coral mounds are interpreted to reflect a hierarchy of three different patterns (*first-* to *third-order*) controlled by the interplay of the regional oceanography, the seafloor topography, and the local hydrodynamic regime. While the *first-order* pattern addressing the large-scale coral mound distribution is steered by the overall slope topography and the water column structure and results in an alongslope organization of the coral mounds within the entire CMP, the *second-order* pattern addressing the small-scale mound distribution is controlled by the underlying topography. In addition, the impact of the local hydrodynamic

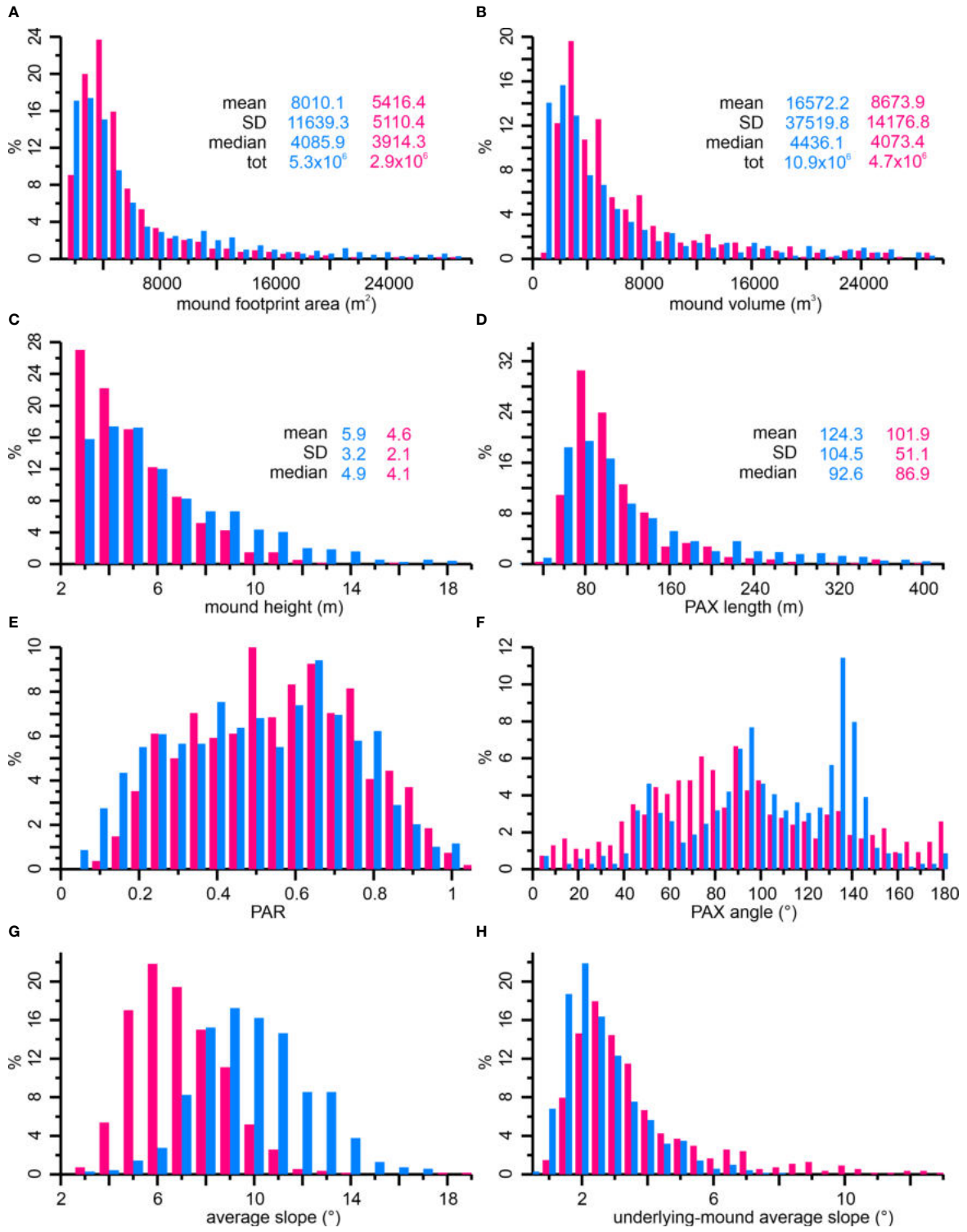

FIGURE 6
Histogram plots showing the relative distribution of selected morphometric parameters collected from the Squid Mounds (light blue) and Coral Belt Mounds (pink): **(A)** mound footprint area (bin size: 1000 m^2), **(B)** mound volume (bin size: 1000 m^3), **(C)** mound height (bin size: 1 m), **(D)** PAX length (bin size: 20 m), **(E)** PAR (bin size: 0.05), **(F)** PAX angle (bin size: 5°), **(G)** average slope of the mounds (bin size: 0.5°), **(H)** average slope of topography underlying the mounds (bin size: 0.5°). Descriptive statistics (mean, standard deviation (SD) and median) are provided for all morphometric data. Further details (description, unit and range) on morphometric parameters are presented in Table 1.

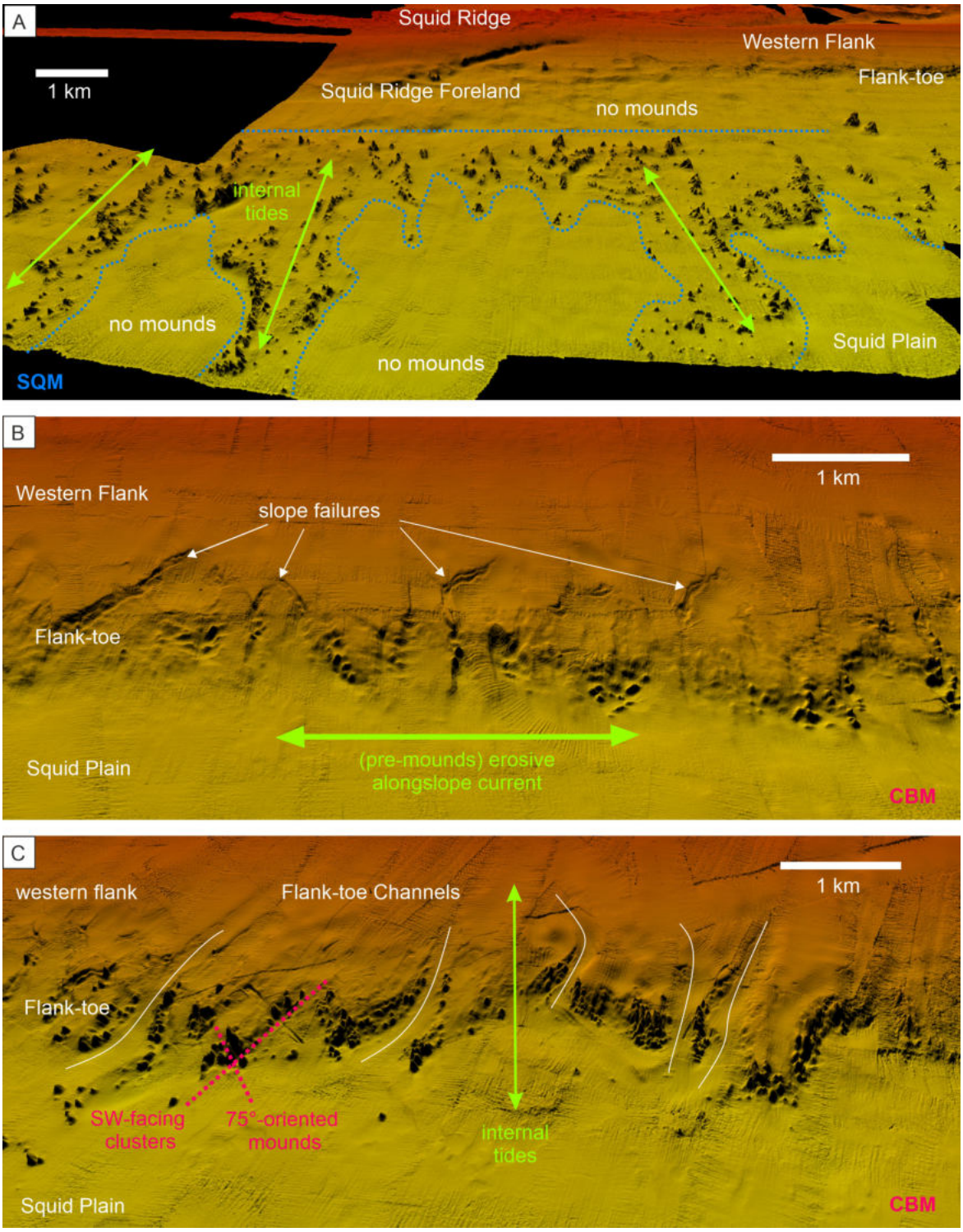

FIGURE 7
Detailed 3D-view of topographic features associated with the Namibian coral mounds. **(A)** 3D-view of the Squid Mounds (SQM). The blue dashed line marks the occurrence of SQM from the surrounding areas with no mounds **(B)** Slope failures appear to be associated with the underlying topography of the northernmost Coral Belt Mounds (CBM). **(C)** Channels (white lines) indenting the Flank-toe with coral mounds along their edges. Vertical exaggeration: 10x. The locations of these examples are shown in Figure 1.

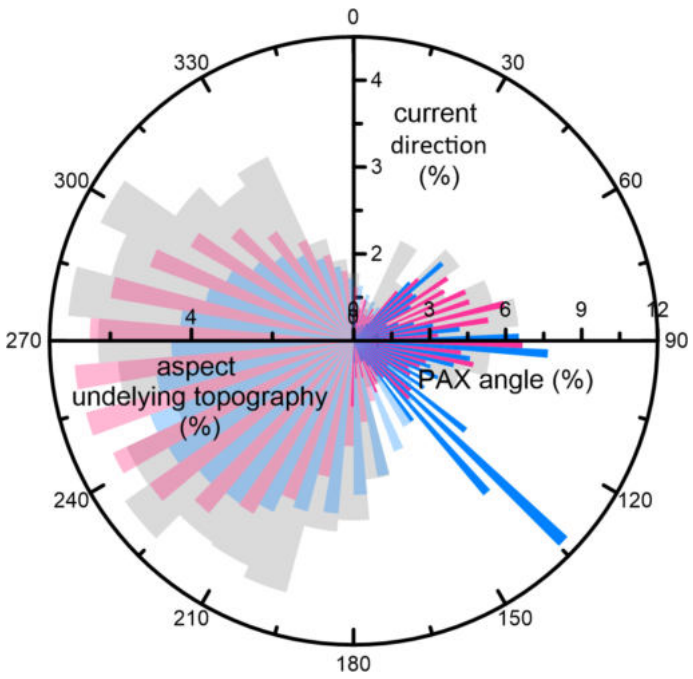

FIGURE 8
Rose diagram with percentages of PAX angle (full colors) and aspect of underlying topography (transparent colors) of Squid Mounds (light blue) and Coral Belt Mounds (pink). In addition, the local bottom current direction among the CBM (collected over 8 days, Hanz et al., 2019) are shown in light gray. Bin size: 10°.

regime and of internal tides creates the *third-order* pattern at the individual mound scale impacting on mound shape and orientation. As mentioned above, previous studies on other CMPs have partially identified similar patterns in the distribution of coral mounds (e.g., De Mol et al., 2002; Fosså et al., 2005; White and Dorschel, 2010; Lim et al., 2018; Hebbeln et al., 2019).

Morphometric variability

Coral mounds or ridges can reach heights of >350 m above the surrounding seafloor (Kenyon et al., 2003) and stretch laterally of >10 km (Colman et al., 2005; Hebbeln et al., 2020). Whereas large coral mounds are comparably easy to detect (e.g., Hovland et al., 1994; Kenyon et al., 1998; De Mol et al., 2002; Beyer et al., 2003; Colman et al., 2005), only recent technological advances in deep-sea acoustic mapping allowed the detection and mapping of small coral mounds (even with heights of <5 m) (e.g., Correa et al., 2012b; De Clippele et al., 2017a; Diesing and Thorsnes, 2018; Lim et al., 2018), also facilitating the detection of new CMPs (e.g., Hebbeln et al., 2014; Lo Iacono et al., 2014; Somoza et al., 2014; Glogowski et al., 2015; Hebbeln et al., 2019; Steinmann et al., 2020), including the Namibian coral mounds (Tamborrino et al., 2019). With a maximum mound height of ca. 20 m and the majority of mounds (83%) having heights of <8 m, the Namibian coral mounds are clearly among the smallest coral mounds discovered so far. Nevertheless, other large CMPs also comprising hundreds to even thousands of individual mounds have similar or only slightly larger mound heights (Magellan mounds, Irish margin, Huvenne et al., 2003; e.g., Florida Straits, Correa et al., 2012b; Atlantic Morocco, Hebbeln et al., 2019). The exponential decrease of mound numbers with increasing mound sizes (Figure 6) has been observed earlier for coral mounds (Correa et al., 2012b) as well as for other carbonate geobodies ranging from shallow-water shoals, to reefs, to karst terrain (Purkis et al., 2010; Harris et al., 2011; Purkis et al., 2016; Purkis and Harris, 2017; Harris et al., 2018).

Initial settlement and widespread occurrence of CWC at several sites might correspond to the high number of small mounds, which likely decreased in the course of mound development as two or more mounds have merged into larger and more complex mound structures (De Mol et al., 2005; Huvenne et al., 2005). Indeed, the small size and the high number of the Namibian mounds clearly indicate multiple initiation sites. Their small sizes are probably related to the relative short mound formation interval (~5 kyr, Tamborrino et al., 2019), which in most cases was probably too short to allow

for the merging of two or more mounds, as it also has been hypothesized for the small Moira Mounds on the Irish margin (Wheeler et al., 2011).

Overall, the coral mounds in both sub-provinces off Namibia exhibit a high morphometric similarity (Figures 6A–D), though there are also a few but distinct differences between the SQM and CBM. The examination of size parameters shows that the total footprint area ($5.7x10^6$ m^2) and volume ($10.9x10^6$ m^3) of the SQM are ~2 times greater than those of the CBM ($2.9x10^6$ m^2; $5.3x10^6$ m^3), despite the comparably minor difference in population size (SQM; 659 mounds, CBM: 542 mounds). Furthermore, the mean, the median and the variability (i.e., standard deviation) are higher in SQM compared to CBM not only for the footprint area and volume but also for the height and PAX length (Figures 6A–D). The height difference between the sub-provinces becomes especially conspicuous for mound heights >8 m, which are reached by 23% of the SQM but only by 8% of the CBM. These observations reveal the occurrence of some larger, higher, and more voluminous SQM that have hardly any counterparts among the CBM (Figure 6).

Mound-shape parameters exhibit that there is a larger number of elongated mounds with PAR of <0.3 among the SQM (21%) compared to the CBM (16%; Figure 6E). This pattern goes along with larger PAX lengths of SQM relative to CBM – 23% of SQM exceed a PAX length of 150 m, which is only reached by12% of the CBM (Figure 6D). A cross-plot of PAX length versus mound height shows that PAX length increase progressively faster than height (Figure 9A) and comparing PAX length versus PAR exhibits that PAR decrease with increasing length (Figure 9C). These results clearly suggest that the Namibian mounds tend to form laterally without gaining substantial additional height, a pattern that is most obvious for the largest SQM (Figure 9C).

The mound elongation becomes most apparent when PAX lengths of ~150 m and heights of ~8 m are exceeded and likely reflects the preferential coral growth on mound flanks facing a favorable hydrodynamic regime (e.g., Messing et al., 1990; Freiwald et al., 1997; Correa et al., 2012b; Mienis et al., 2014; Cathalot et al., 2015; De Clippele et al., 2017b; Lim et al., 2017). However, some of these elongated mounds might result from the merging of smaller mounds (see Figure 2). This merging could be facilitated by the high-density of mounds (Figure 5A) and the alignment of coral mounds along underlying topographic features that are also largely oriented downslope (*second-order* pattern, Figures 5B, 7, 8). The lack of large elongated mounds in the CBM sub-province (Figure 9C) suggests that the two sub-provinces were subject to (slightly) different forcing, which favored the merging of mounds in SQM. Possible forcing factors could be, e.g., slightly better living conditions for CWC on the SQM enabling faster formation or shorter distances between "early-stage" mounds facilitating earlier merging.

The evaluation of coral mound orientation shows variable PAX angles of smaller mounds (comprising the majority of the CBM and many SQM). This might be ascribed to their more circular mound footprint areas (PAR, Figure 9C) and an additional influence of the underlying topography on their orientation (PAX angles, Figure 6F), which could result in mound orientations completely unrelated to the hydrodynamic regime, as observed by the PAX angles of early-stage coral mounds developing on carbonate blocks/boulders in the Florida Straits (Correa et al., 2012b; Hebbeln et al., 2012). In contrast, larger coral mounds with heights >~8 m and PAX lengths >~150 m (mostly SQM) exhibit a preferential PAX orientation that narrows towards ~90° with increasing size (Figures 9D, E). This preferred PAX orientation of ~90°, is roughly parallel to the modern local tidal regime (Hanz et al., 2019), which suggests an increasingly hydrodynamic control on the shape of the mounds.

The average slope is a morphometric parameter strongly dependent on mound height, as it is, for example, shown by the consistent parallel increase of mound height and average slope (Figure 9B). This is interpreted to reflect the gain of relief from the surrounding seafloor during the early mound formation stage. With increasing height, the local hydrodynamic regime strengthened around the mound summit resulting in an enhanced lateral food supply to the CWC there – as also implicated in the development of shallow-water reefs (Schlager and Purkis, 2013). This is supported by the common observation from various CMPs in which CWC predominantly thrive on mound tops (e.g., Huvenne et al., 2005; Wienberg et al., 2008; Le Guilloux et al., 2009; Heindel et al., 2010; Westphal et al., 2012).

Whereas the elongation and direction of individual mounds are probably largely controlled by hydrodynamics, the interplay of the duration of the formation period and the mound formation rate might play a key role for the size parameters, as suggested by Mortensen et al. (2001). Excluding the large (most likely merged) SQM, the populations of SQM and CBM have very similar size-frequency distributions (Figure 6). Considering the relative shallow occurrence and post-glacial development of the Namibian mounds combined with the synchronous demise of the CWC in both sub-provinces (Tamborrino et al., 2019), suggests that similar mound sizes in the sub-provinces likely correspond to a similar temporal development (quasi-synchronous initiation and akin formation rates). Thus, probably only small offsets, e.g., in the environmental factors supporting CWC or in the initial distance between mounds, controlled the small differences between SQM and CBM, most prominently expressed by the more frequent merging of mounds in the SQM sub-province.

The relationship between mound height and PAX length from the Namibian mounds follows a common trend in coral mound development, identifiable also in other CMPs, for which instead of PAX lengths partly comparable measures, such as mound length or max diameter of the mound footprint area have been used. The overall ratio of mound height to PAX length measured for the Namibian coral mounds is <0.2 (98% is

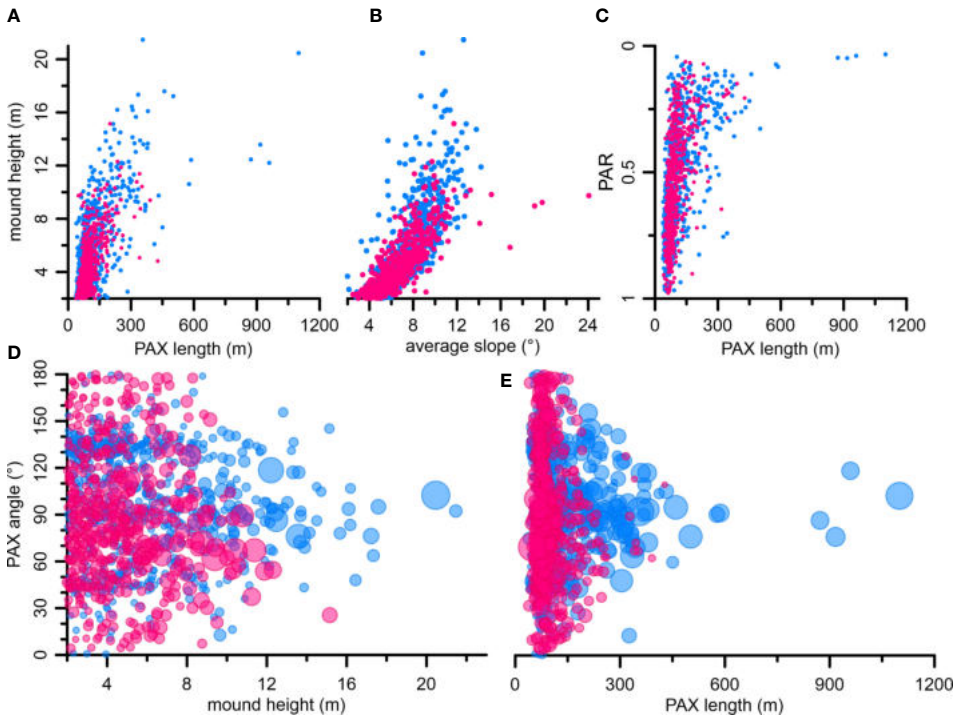

FIGURE 9
(A, B) Crossplots with mound height versus PAX length **(A)** and average slope **(B)**. **(C)** Crossplot with PAR versus PAX length (descending order for the y-axis). **(D, E)** Crossplots with mound height and PAX length versus PAX angle. Size of the dots is proportional to the PAX length **(D)** and mound height **(E)**. Color: light blue, Squid Mounds; pink, Coral Belt Mounds.

even <0.1), comparable with the (mean) values of height and PAX-like parameters measured from other CMPs (e.g., Huvenne et al., 2003; Wheeler et al., 2007; Wheeler et al., 2008; Lo Iacono et al., 2014; Hebbeln et al., 2019). These low ratios highlight the "shield-like" morphology of most coral mounds rather than the conical morphology often described in the literature (e.g., van Rooij et al., 2003; Wheeler et al., 2007). This latter term most likely results from the vertical exaggeration often applied to seabed maps and seismic sections, which can visually transfer a shield-like to a conical morphology.

Finally, the coral mound development off Namibia from small, rather round mounds with variable orientations and relative flat slopes towards larger elongated mounds with preferred orientations and steeper slopes supports the hypothesis of Wheeler et al. (2007) about "inherited" and "developed" mound morphologies. As pointed out above, this transition from the small "inherited" to the larger "developed" mounds probably reflects the increasing control of the local hydrodynamic regime on the formation of mounds. Furthermore, based on the observed transition of the rather "inherited" to a predominantly "developed" mound morphology at a mound height of ~8 m and a PAX length of ~150 m, we postulate these values as size thresholds for the transition from "inherited" to "developed" coral mounds. If these thresholds are valid for this region only or reflect general thresholds must be tested in the future at other CMPs.

Carbonate deposition in the Namibian mounds

The morphometric analyses also allow the calculation of mound volumes (Figure 6B). Based on this calculation, the total volume of the Namibia coral mounds is estimated to be 16.2×10^6 m^3 (SQM: $10.9x10^6$ m^3; CBM: $5.3x10^6$ m^3). These values are a conservative estimate as mounds with a footprint area of <900 m^2 or height of <2 m are not considered, and the mapped area likely does not cover the entire extent of the Namibian CMP. Following the approach of Hebbeln et al. (2019), the stored coral carbonate within the Namibian mounds is estimated by using the following assumptions: based on a volume ratio of 20 vol.% CWC to 80 vol.% matrix sediment (Titschack et al., 2015; Titschack et al., 2016) and applying average density values for coral aragonite of ~2.66 g cm^{-3} and for matrix sediments of 1.52 g cm^{-3} (Hamilton, 1976; Dorschel et al., 2007), the average sediment density of the coral mounds is estimated to be ~1.75 g cm^{-3} with a 30 wt.% contribution of CWC. Based on these assumptions, the total mass of the Namibian mounds is calculated to 28.2×10^6 tons to which

CWC contribute 8.5 × 10^6 tons of carbonate. Considering a mound development period lasting for ~5 kyr (Tamborrino et al., 2019), the CWC-related carbonate production of the Namibian coral mounds had a rate of ~1,900 tons yr^{-1}, which is very close to the number of ~1,550 tons yr^{-1} obtained from a large CMP located on the Moroccan slope in the NE Atlantic (ca. 10x volume of the Namibian CMP, Hebbeln et al., 2019). With an extension of ~200 km^2 as derived from the heatmaps (Figure 5), the coral-derived carbonate productivity in the SQM and CBM sub-provinces was approximately 9.5 g m^{-2} yr^{-1} during their development (4.9-9.5 kyr, Tamborrino et al., 2019). These numbers confirm the capacity of the coral mounds to accumulate carbonate much faster (2.5 times) than the surrounding seafloor (Milliman, 1993; Titschack et al., 2009; Titschack et al., 2015; Titschack et al., 2016).

Conclusions

The combined analysis of the spatial distribution of the Namibian coral mounds and their morphometric characteristics enables to outline a potential concept for understanding the initiation and the early development of these mounds. A *first-order* pattern derived from the depth interval, in which CWC could thrive due to the supporting environmental conditions created along a water-mass boundary that stretches along the margin. The *second-order* pattern likely corresponds to the sites colonized by the first pioneering coral planulae, which successfully developed in colonies/patches that are aligned along topographic features at the seafloor which off Namibia are erosive in nature and stretch downslope. Mound orientation represents the *third-order* pattern documenting the increasing hydrodynamic control on mound morphology along their formation. These patterns reflect how environmental conditions, namely the interplay of topography with the regional oceanography and local hydrography, influenced mound development off Namibia at different scales (from colony to coral mound province).

The progressively faster increase in PAX length compared to mound height, especially beyond the thresholds of ~150 m in length and ~8 m in height, probably documents the initial from inherited to developed mounds as this trend aligns with the change from rather random PAX orientations to orientations parallel to the main direction of the tidal bottom current. This is most pronounced for the larger SQM. These numbers can be seen as the first size criteria for the transition from the inherited to the developed mound stage.

This analysis of an extensive morphometric database increases our understanding of the formation of the Namibian coral mounds (incl. e.g. carbonate production) and the involved processes. Similar approaches should be considered for future studies on other CMPs in the Atlantic Ocean (and beyond), which would allow to differentiate between locally unique features and regionally or basin-wide common features of coral mound formation. Such common features to be identified bear a large potential for the definition of a set of basic principles to describe the formation of coral mounds.

Data availability statement

Publicly available datasets were analyzed in this study. This data can be found here: https://doi.pangaea.de/10.1594/PANGAEA.944627 (Squid Mounds) and https://doi.pangaea.de/10.1594/PANGAEA.944595 (Coral Belt Mounds).

Author contributions

LT wrote the paper, carried out the spatial-morphometric analyses, prepared the figures and the supplemental material. LT, JT, DH, and CW conceived the work. DH and CW coordinated the scientific cruise and the collection of the datasets utilized for the manuscript. LT and JT processed the hydroacoustic data. GE and SP provided fundamental support for the morphometric analyses. All the authors discussed the results and contributed to the manuscript. All the authors have stated their agreement with the present version of the manuscript.

Funding

This research was supported by the German Academic Exchange Service (DAAD; LT), the German Science Foundation (DH, CW), and the Cluster of Excellence 'The Ocean Floor – Earth's Uncharted Interface' (EXC-2077–390741603; JT).

Acknowledgments

We thank the officers and the crew of the *RV Meteor*, the Shipboard Scientific Party and the German Diplomatic Corps for the substantial support for the cruise M112 ANNA. We thank Schlumberger for providing the license of Petrel™ software to University of Miami, Furu Mienis and Ulrike Hanz (NIOZ) are thanked for providing the datasets collected by the benthic lander. Paul Wintersteller, Stefanie Gaide (MARUM), Manuel Jesus Roman Alpiste (CSIC, IACT, Granada) and Débora Duarte (Royal Holloway, University of London) are thanked for the support with the hydroacoustic data. The data reported in this paper are archived in Pangea (www.pangea.de).

Conflict of interest

The authors declare that the research was conducted in the absence of any commercial or financial relationships that could be construed as a potential conflict of interest.

Publisher's note

References

Angeletti, L., Castellan, G., Montagna, P., Remia, A., and Taviani, M. (2020). The "Corsica channel cold-water coral province" (Mediterranean Sea). *Front. Mar. Sci.* 7. doi: doi.org/10.3389/fmars.2020.00661

Bøe, R., Bellec, V. K., Dolan, M. F. J., Buhl-Mortensen, P., Rise, L., and Buhl-Mortensen, L. (2016). Cold-water coral reefs in the hola glacial trough off vesterålen, north Norway. *Geological Society London Memoirs* 46, 309–310. doi: 10.1144/M46.8

Bartzke, G., Siemann, L., Büssing, R., Nardone, P., Koll, K., Hebbeln, D., et al. (2021). Investigating the prevailing hydrodynamics around a cold-water coral colony using a physical and a numerical approach. *Front. Mar. Sci.* 8. doi: 10.3389/fmars.2021.663304

Beyer, A., Schenke, H. W., Klenke, M., and Niederjasper, F. (2003). High resolution bathymetry of the eastern slope of the porcupine seabight. *Mar. Geology* 198, 27–54. doi: 10.1016/S0025-3227(03)00093-8

Boolukos, C. M., Lim, A., O'riordan, R. M., and Wheeler, A. J. (2019). Cold-water corals in decline – a temporal (4 year) species abundance and biodiversity appraisal of complete photomosaiced cold-water coral reef on the Irish margin. *Deep Sea Res. Part I: Oceanographic Res. Papers* 146, 44–54. doi: 10.1016/j.dsr.2019.03.004

Buhl-Mortensen, L., Serigstad, B., Buhl-Mortensen, P., Olsen, M. N., Ostrowski, M., Błażewicz-Paszkowycz, M., et al. (2017). First observations of the structure and megafaunal community of a large lophelia reef on the ghanaian shelf (the gulf of Guinea). *Deep Sea Res. Part II: Topical Stud. Oceanography* 137, 148–156. doi: 10.1016/j.dsr2.2016.06.007

Cacchione, D., Pratson, L. F., and Ogston, A. (2002). The shaping of continental slopes by internal tides. *Science* 296, 724–727. doi: 10.1126/science.1069803

Caress, D. W., and Chayes, D. (1995). "New software for processing sidescan data from sidescan-capable multibeam sonars," in *Challenges for Our Global Environment: Conference Proceedings, Oceans '95 MTS/IEEE*. 2, 997–10000. doi: 10.1109/OCEANS.1995.528558

Carranza, A., Recio, A. M., Kitahara, M., Scarabino, F., Ortega, L., López, G., et al. (2012). Deep-water coral reefs from the Uruguayan outer shelf and slope. *Mar. Biodiversity* 42, 411–414. doi: 10.1007/s12526-012-0115-6

Cathalot, C., Van Oevelen, D., Cox, T. J. S., Kutti, T., Lavaleye, M., Duineveld, G., et al. (2015). Cold-water coral reefs and adjacent sponge grounds: hotspots of benthic respiration and organic carbon cycling in the deep sea. *Front. Mar. Sci.* 2. doi: 10.3389/fmars.2015.00037

Cheriton, O. M., Mcphee-Shaw, E. E., Shaw, W. J., Stanton, T. P., Bellingham, J. G., and Storlazzi, C. D. (2014). Suspended particulate layers and internal waves over the southern Monterey bay continental shelf: An important control on shelf mud belts? *J. Geophysical Research: Oceans* 119, 428–444. doi: 10.1002/2013JC009360

Collart, T., Verreydt, W., Hernández-Molina, F. J., Llave, E., León, R., Gómez-Ballesteros, M., et al. (2018). Sedimentary processes and cold-water coral mini-mounds at the Ferrol canyon head, NW Iberian margin. *Prog. Oceanogr.* 169, 48–65. doi: 10.1016/j.pocean.2018.02.027

Colman, J. G., Gordaon, D. M., Lane, A. P., Forde, M. J., and Fitzpatrick, J. (2005). "Carbonate mounds off mauretania, Northwest Africa: status of deep-water corals and implications for management of fishing and oil exploration activities," in *Cold-water corals and ecosystems*. Eds. A. Freiwald and J. M. Roberts (Berlin-Heidelberg: Springer), 417–441.

Corbera, G., Lo Iacono, C., Gràcia, E., Grinyó, J., Pierdomenico, M., Huvenne, V., et al. (2019). Ecological characterisation of a Mediterranean cold-water coral reef: Cabliers coral mound province (Alboran Sea, western Mediterranean). *Prog. Oceanography* 175, 245–262. doi: 10.1016/j.pocean.2019.04.010

Correa, T. B. S., Eberli, G. P., Grasmueck, M., Reed, J. K., and Correa, A. M. S. (2012a). Genesis and morphology of cold-water coral ridges in a unidirectional current regime. *Mar. Geology* 326–328, 14–27. doi: 10.1016/j.margeo.2012.06.008

Correa, T. B. S., Grasmueck, M., Eberli, G. P., Reed, J. K., Verwer, K., and Purkis, S. (2012b). Variability of cold-water coral mounds in a high sediment input and tidal current regime, straits of Florida. *Sedimentology* 59, 1278–1304. doi: 10.1111/j.1365-3091.2011.01306.x

Davies, A. J., Duineveld, G., Lavaleye, M., Bergman, M. J., Van Haren, H., and Roberts, J. M. (2009). Downwelling and deep-water bottom currents as food supply mechanisms to the cold-water coral *Lophelia pertusa* (Scleractinia) at the mingulay reef complex. *Limnol. Oceanogr.* 54, 620–629. doi: 10.4319/lo.2009.54.2.0620

Davies, A. J., and Guinotte, J. M. (2011). Global habitat suitability for framework-forming cold-water corals. *PloS One* 6, e18483. doi: 10.1371/journal.pone.0018483

Davies, A. J., Wisshak, M., Orr, J. C., and Roberts, J. M. (2008). Predicting suitable habitat for the cold-water coral *Lophelia pertusa* (Scleractinia). *Deep-Sea Res. I* 55, 1048–1062. doi: 10.1016/j.dsr.2008.04.010

De Clippele, L. H., Gafeira, J., Robert, K., Hennige, S., Lavaleye, M. S., Duineveld, G. C. A., et al. (2017a). Using novel acoustic and visual mapping tools to predict the small-scale spatial distribution of live biogenic reef framework in cold-water coral habitats. *Coral Reefs* 36, 255–268. doi: 10.1007/s00338-016-1519-8

De Clippele, L. H., Huvenne, V., Orejas, C., Lundälv, T., Fox, A., Hennige, S. J., et al. (2017b). The effect of local hydrodynamics on the spatial extent and morphology of cold-water coral habitats at tisler reef, Norway. *Coral Reefs* 37, 253–266. doi: 10.1007/s00338-017-1653-y

De Clippele, L. H., Rovelli, L., Ramiro-Sánchez, B., Kazanidis, G., Vad, J., Turner, S., et al. (2021). Mapping cold-water coral biomass: an approach to derive ecosystem functions. *Coral Reefs* 40, 215–231. doi: 10.1007/s00338-020-02030-5

De Haas, H., Mienis, F., Frank, N., Richter, T. O., Steinbacher, R., De Stigter, H., et al. (2009). Morphology and sedimentology of (clustered) cold-water coral mounds at the south rockall trough margins, NE Atlantic ocean. *Facies* 55, 1–26. doi: 10.1007/s10347-008-0157-1

De Mol, B., Henriet, J.-P., and Canals, M. (2005). ""Development of coral banks in the porcupine seabight: do they have Mediterranean ancestors?"," in *Cold-water corals and ecosystems*. Eds. A. Freiwald and J. M. Roberts (Berlin-Heidelberg: Springer), 515–533.

De Mol, B., Kozachenko, M., Wheeler, A. J., Alvares, H., Henriet, J.-P., and Olu-Le Roy, K. (2007). Thérèse mound: a case study of coral bank development in the belgica mound province, porcupine seabight. *Earth Planetary Sci. Lett.* 96, 103–120. doi: doi.org/10.1016/S0025-3227(02)00281-5

De Mol, B., Van Rensbergen, P., Pillen, S., Van Herreweghe, K., Van Rooij, D., Mcdonnell, A., et al. (2002). Large Deep-water coral banks in the porcupine basin, southwest of Ireland. *Mar. Geology* 188, 193–231. doi: 10.1016/S0025-3227(02)00281-5

Diesing, M., and Thorsnes, T. (2018). Mapping of cold-water coral carbonate mounds based on geomorphometric features: an object-based approach. *Geosciences* 8, 34. doi: 10.3390/geosciences8020034

Dodds, L. A., Black, K. D., Orr, H., and Roberts, J. M. (2009). Lipid biomarkers reveal geographical differences in food supply to the cold-water coral *Lophelia pertusa* (Scleractinia). *Mar. Ecol. Prog. Ser.* 397, 113–124. doi: 10.3354/meps08143

Dorschel, B., Hebbeln, D., Rüggeberg, A., and Dullo, C. (2007). Carbonate budget of a cold-water coral carbonate mound: Propeller mound, porcupine seabight. *Int. J. Earth Sci.* 96, 73–83. doi: 10.1007/s00531-005-0493-0

Douarin, M., Elliot, M., Noble, S. R., Sinclair, D., Henry, L.-A., Long, D., et al. (2013). Growth of north-east Atlantic cold-water coral reefs and mounds during the Holocene: A high resolution U-series and ^{14}C chronology. *Earth Planetary Sci. Lett.* 375, 176–187. doi: 10.1016/j.epsl.2013.05.023

Duineveld, G. C. A., Jeffreys, R. M., Lavaleye, M. S. S., Davies, A. J., Bergman, M. J. N., Watmough, T., et al. (2012). Spatial and tidal variation in food supply to shallow cold-water coral reefs of the mingulay reef complex (Outer Hebrides, Scotland). *Mar. Ecol. Prog. Ser.* 444, 97–115. doi: 10.3354/meps09430

Duineveld, G., Lavaleye, M., Bergman, M., De Stigter, H., and Mienis, F. (2007). Trophic structure of a cold-water coral mound community (Rockall bank, NE Atlantic) in relation to the near-bottom particle supply and current regime. *Bull. Mar. Sci.* 81, 449–467.

Dullo, W.-C., Flögel, S., and Rüggeberg, A. (2008). Cold-water coral growth in relation to the hydrography of the celtic and Nordic European continental margin. *Mar. Ecol. Prog. Ser.* 371, 165–176. doi: 10.3354/meps07623

Fosså, J. H., Lindberg, B., Christensen, O., Lundälv, T., Svellingen, I., Mortensen, P. B., et al. (2005). "Mapping of lophelia reefs in Norway: experiences and survey methods," in *Cold-water corals and ecosystems*. Eds. A. Freiwald and J. M. Roberts (Berlin-Heidelberg: Springer), 359–391.

Foubert, A., Beck, T., Wheeler, A. J., Opderbecke, J., Grehan, A., Klages, M., et al. (2005). "New view of the belgica mounds, porcupine, NE Atlantic: preliminary results from the polarstern ARK-XIX/3a ROV cruise," in *Cold-water corals and ecosystems*. Eds. A. Freiwald and J. M. Roberts (Berli-Heidelberg: Springer), 403–415.

Foubert, A., Depreiter, D., Beck, T., Maignien, L., Pannemans, B., Frank, N., et al. (2008). Carbonate mounds in a mud volcano province off north-west Morocco: Key to processes and controls. *Mar. Geol.* 248 (1-2), 74–96. doi: 10.1016/j.margeo.2007.10.012

Frederiksen, R., Jensen, A., and Westerberg, H. (1992). The distribution of the scleractinian coral *Lophelia pertusa* around the faroe islands and the relation to internal tidal mixing. *Sarsia* 77, 157–171. doi: 10.1080/00364827.1992.10413502

Freiwald, A., Henrich, R., and Pätzold, J. (1997). "Anatomy of a deep-water coral reef mound from stjernsund, West-finnmark, northern Norway". In *Cool-water carbonates* Eds. N. P. James and J. A. D. Clarke. (SEPM Special Publications). 56.

Freiwald, A., Wilson, J. B., and Henrich, R. (1999). Grounding pleistocene icebergs shape recent deep-water coral reefs. *Sedimentary Geology* 125, 1–8. doi: 10.1016/S0037-0738(98)00142-0

Galvez, K. C. (2020). *The distribution and growth patterns of cold-water corals in the straits of Florida* (Miami, US: University of Miami).

Garrett, C., and Kunze, E. (2007). Internal tide generation in the deep ocean. *Annu. Rev. Fluid Mechanics* 39, 57–87. doi: 10.1146/annurev.fluid.39.050905.110227

Geissler, W. H., Schwenk, T., and Wintersteller, P. (2013). *Walvis Ridge Passive-Source Seismic Experiment (WALPASS) - Cruise No. MSM20/1 - January 06 - January 15, 2012 - Cape Town (South Africa) - Walvis Bay (Namibia)*. MARIA S. MERIAN-Berichte, DFG-Senatskommission für Ozeanographie, MSM20/1, 54 pp.

Genin, A., Dayton, P. K., Lonsdale, P. F., and Spiess, F. N. (1986). Corals on seamount peaks provide evidence of current acceleration over deep-sea topography. *Nature* 322, 59–61. doi: 10.1038/322059a0

Giraudeau, J., Bailey, G. W., and Pujol, C. (2000). A high-resolution time-series analyses of particle fluxes in the northern benguela coastal upwelling system: carbonate record of changes in biogenic production and particle transfer processes. *Deep Sea Res. Part II: Topical Stud. Oceanogr.* 47, 1999–2028. doi: 10.1016/S0967-0645(00)00014-X

Glogowski, S., Dullo, W. C., Feldens, P., Liebetrau, V., Von Reumont, J., Hühnerbach, V., et al. (2015). The eugen seibold coral mounds offshore western Morocco: oceanographic and bathymetric boundary conditions of a newly discovered cold-water coral province. *Geo-Marine Lett.* 35, 257–269. doi: 10.1007/s00367-015-0405-7

Grasmueck, M., Eberli, G. P., Viggiano, D. A., Correa, T., Rathwell, G., and Luo, J. (2006). Autonomous underwater vehicle (AUV) mapping reveals coral mound distribution, morphology, and oceanography in deep water of the straits of Florida. *Geophysical Res. Lett.* 33, L23616. doi: 10.1029/2006GL027734

Haberkern, J. (2017). *Contouritic depositional systems influenced by complex seafloor topography - late Cenozoic seismoacoustic reconstructions from the Galicia and Angola continental margins* (Bremen, Germany: University of Bremen).

Hamilton, E. L. (1976). Variations of density and porosity with depth in deep-sea sediments. *J. Sedimentary Res.* 46, 280–300. doi: 10.1306/212F6F3C-2B24-11D7-8648000102C1865D

Hanz, U., Wienberg, C., Hebbeln, D., Duineveld, G., Lavaleye, M., Juva, K., et al. (2019). Environmental factors influencing benthic communities in the oxygen minimum zones on the Angolan and Namibian margins. *Biogeosciences* 16, 4337–4356. doi: 10.5194/bg-16-4337-2019

Harris, P. M., Purkis, S. J., and Ellis, J. (2011). Analyzing spatial patterns in modern carbonate sand bodies from great bahama bank. *J. Sedimentary Res.* 81, 185–206. doi: 10.2110/jsr.2011.21

Harris, P., Purkis, S., and Reyes, B. (2018). Statistical pattern analysis of surficial karst in the pleistocene Miami oolite of south Florida. *Sedimentary Geology* 367, 84–95. doi: 10.1016/j.sedgeo.2018.02.002

Hebbeln, D. (2019). "8 highly variable submarine landscapes in the alborán Sea created by cold-water corals,," in *Mediterranean Cold-water corals: Past, present and future: Understanding the deep-Sea realms of coral*. Eds. C. Orejas and C. Jiménez (Cham: Springer International Publishing), 61–65.

Hebbeln, D., Bender, M., Gaide, S., Titschack, J., Vandorpe, T., Van Rooij, D., et al. (2019). Thousands of cold-water coral mounds along the Moroccan Atlantic continental margin: Distribution and morphometry. *Mar. Geology* 411, 51–61. doi: 10.1016/j.margeo.2019.02.001

Hebbeln, D., Wienberg, C.And Cruise Participants (2012). "Report and preliminary results of R/V MARIA s. MERIAN cruise MSM20-4. WACOM. Bridgetown-Freeport, 14.03.-07.04.2012," in *Reports dept of geosciences vol. 290* (Bremen, Germany: Univ of Bremen).

Hebbeln, D., Wienberg, C., Bender, M., Bergmann, F., Dehning, K., Dullo, W.-C., et al. (2017). *ANNA - cold-water coral ecosystems off Angola and namibia. cruise M122 – December 30, 2015 – January 31, 2016 – Walvis bay (Namibia) – Walvis bay (Namibia)*. 66, DFG-Senatskommission für Ozeanographie. Bremen: METEOR-Berichte

Hebbeln, D., Wienberg, C., Dullo, W.-C., Freiwald, A., Mienis, F., Orejas, C., et al. (2020). Cold-water coral reefs thriving under hypoxia. *Coral Reefs* 39, 853–859. doi: 10.1007/s00338-020-01934-6

Hebbeln, D., Wienberg, C., Wintersteller, P., Freiwald, A., Becker, M., Beuck, L., et al. (2014). Environmental forcing of the campeche cold-water coral province, southern gulf of Mexico. *Biogeosciences* 11, 1799–1815. doi: 10.5194/bg-11-1799-2014

Heindel, K., Titschack, J., Dorschel, B., Huvenne, V., and Freiwald, A. (2010). The sediment composition and predictive mapping of facies on the propeller mound–a cold-water coral mound (Porcupine seabight, NE Atlantic). *Continental Shelf Res.* 30, 1814–1829. doi: 10.1016/j.csr.2010.08.007

Hennige, S. J., Larsson, A. I., Orejas, C., Gori, A., De Clippele, L. H., Lee, Y. C., et al. (2021). Using the goldilocks principle to model coral ecosystem engineering. *Proc. R. Soc. B: Biol. Sci.* 288, 20211260. doi: 10.1098/rspb.2021.1260

Horn, B. K. (1981). Hill shading and the reflectance map. *Proc. IEEE* 69, 14–47. doi: 10.1109/PROC.1981.11918

Hosegood, P., Bonnin, J., and Van Haren, H. (2004). Solibore-induced sediment resuspension in the Faeroe-Shetland channel. *Geophysical Res. Lett.* 31, L09301. doi: 10.1029/2004GL019544

Hovland, M., Farestveit, R., and Mortensen, P. B. (1994). "Large cold-water coral reefs off mid-Norway - a problem for pipe-laying?" *Conference Proceedings (3), Oceanology International*. pp. 8-11

Hübscher, C., Dullo, C., Flögel, S., Titschack, J., and Schönfeld, J. (2010). Contourite drift evolution and related coral growth in the eastern gulf of Mexico and its gateways. *Int. J. Earth Sci.* 99, 191–206. doi: 10.1007/s00531-010-0558-6

Huvenne, V., Beyer, A., De Haas, H., Dekindt, K., Henriet, J.-P., Kozachenko, M., et al. (2005). "The seabed appearance of different coral bank provinces in the porcupine seabight, NE Atlantic: results from sidescan sonar and ROV seabed mapping," in *Cold-water corals and ecosystems*. Eds. A. Freiwald and J. M. Roberts (Heidelberg: Springer), 535–569.

Huvenne, V., De Mol, B., and Henriet, J.-P. (2003). A 3D seismic study of the morphology and spatial distribution of buried coral banks in the porcupine basin, SW of Ireland. *Mar. Geology* 198, 5–25. doi: 10.1016/S0025-3227(03)00092-6

Inthorn, M., Mohrholz, V., and Zabel, M. (2006). Nepheloid layer distribution in the benguela upwelling area offshore Namibia. *Deep Sea Res. Part I: Oceanogr. Res. Papers* 53, 1423–1438. doi: 10.1016/j.dsr.2006.06.004

Kenyon, N. H., Akhmetzhanov, A. M., Wheeler, A. J., Van Weering, T. C. E., De Haas, H., and Ivanov, M. K. (2003). Giant carbonate mud mounds in the southern rockall trough. *Mar. Geology* 195, 5–30. doi: 10.1016/S0025-3227(02)00680-1

Kenyon, N., Ivanov, M., and Akhmetzhanov, A. (1998). Cold water carbonate mounds and sediment transport on the northeast Atlantic margin - preliminary results of geological and geophysical investigations during the TTR-7 cruise of R/V professor logachev. 52, 177

Kiriakoulakis, K., Harper, E., and Wolff, G. A. (2005). "Lipids and nitrogeen isotopes of two deep-water corals from the north-East Atlantic: initial results and implications for their nutrition," in *Cold-water corals and ecosystems*. Eds. A. Freiwald and J. M. Roberts (Berlin-Heidelberg: Springer), 715–729.

Klymak, J. M., Alford, M. H., Pinkel, R., Lien, R.-C., Yang, Y. J., and Tang, T.-Y. (2011). The breaking and scattering of the internal tide on a continental slope. *J. Phys. Oceanogr.* 41, 926–945. doi: 10.1175/2010JPO4500.1

Lavaleye, M., Duineveld, G., Lundälv, T., White, M., Guihen, D., Kiriakoulakis, K., et al. (2009). Cold-water corals on the tisler reef: Preliminary observations on the dynamic reef environment. *Oceanography* 22, 76–84. doi: 10.5670/oceanog.2009.08

Le Guilloux, E., Olu, K., Bourillet, J. F., Savoye, B., Iglésias, S. P., and Sibuet, M. (2009). First observations of deep-sea coral reefs along the Angola margin. *Deep Sea Res. Part II: Topical Stud. Oceanogr.* 56, 2394–2403. doi: 10.1016/j.dsr2.2009.04.014

Lim, A., Huvenne, V., Vertino, A., Spezzaferri, S., and Wheeler, A. J. (2018). New insights on coral mound development from groundtruthed high-resolution ROV-mounted multibeam imaging. *Mar. Geology* 403, 225–237. doi: 10.1016/j.margeo.2018.06.006

Lim, A., Wheeler, A. J., and Arnaubec, A. (2017). High-resolution facies zonation within a cold-water coral mound: The case of the piddington mound, porcupine seabight, NE Atlantic. *Mar. Geology* 390, 120–130. doi: 10.1016/j.margeo.2017.06.009

Lim, A., Wheeler, A. J., and Conti, L. (2021). Cold-water coral habitat mapping: trends and developments in acquisition and processing methods. *Geosciences* 11 (1), 9. doi: 10.3390/geosciences11010009

Lindberg, B., Berndt, C., and Mienert, J. (2007). The fugløy reef at 70°N; acoustic signature, geologic, geomorphologic and oceanographic setting. *Int. J. Earth Sci.* 96, 201–213. doi: 10.1007/s00531-005-0495-y

Lo Iacono, C., Gràcia, E., Ranero, C. R., Emelianov, M., Huvenne, V., Bartolomé, R., et al. (2014). The West melilla cold water coral mounds, Eastern alboran Sea: Morphological characterization and environmental context. *Deep-Sea Res. Part II: Topical Stud. Oceanogr.* 99, 316–326. doi: 10.1016/j.dsr2.2013.07.006

López Correa, M., Montagna, P., Joseph, N., Rüggeberg, A., Fietzke, J., Flögel, S., et al. (2012). Preboreal onset of cold-water coral growth beyond the Arctic circle revealed by coupled radiocarbon and U-series dating and neodymium isotopes. *Quaternary Sci. Rev.* 34, 24–43. doi: 10.1016/j.quascirev.2011.12.005

Mareano (2020) *Coral reefs off Norway*. Available at: http://mareano.no/kart/mareano_en.html#maps/4738.

Margreth, S., Gennari, G., Rüggeberg, A., Comas, M. C., Pinheiro, L. M., and Spezzaferri, S. (2011). Growth and demise of cold-water coral ecosystems on mud volcanoes in the West alboran Sea: The messages from the planktonic and benthic foraminifera. *Mar. Geology* 282, 26–39. doi: 10.1016/j.margeo.2011.02.006

Masson, D. G., Bett, B. J., Billett, D. S. M., Jacobs, C. L., Wheeler, A. J., and Wynn, R. B. (2003). The origin of deep-water, coral-topped mounds in the northern rockall trough, northeast Atlantic. *Mar. Geology* 194, 159–180. doi: 10.1016/S0025-3227(02)00704-1

Matos, L., Wienberg, C., Titschack, J., Schmiedl, G., Frank, N., Abrantes, F., et al. (2017). Coral mound development at the campeche cold-water coral province, southern gulf of Mexico: Implications of Antarctic intermediate water increased influence during interglacials. *Mar. Geology* 392, 53–65. doi: 10.1016/j.margeo.2017.08.012

Messing, C. G., Neumann, A. C., and Lang, J. C. (1990). Biozonation of deep-water lithoherms and associated hardgrounds in the northeastern straits of Florida. *Palaios* 5, 15–33. doi: 10.2307/3514994

Mienis, F., Bouma, T. J., Witbaard, R., Van Oevelen, D., and Duineveld, G. C. A. (2019). Experimental assessment of the effects of coldwater coral patches on water flow. *Mar. Ecol. Prog. Ser.* 609, 101–117. doi: 10.3354/meps12815

Mienis, F., De Stigter, H. C., De Haas, H., and Van Weering, T. C. E. (2009). Near-bed particle deposition and resuspension in a cold-water coral mound area at the southwest rockall trough margin, NE Atlantic. *Deep Sea Res. I* 56, 1026–1038. doi: 10.1016/j.dsr.2009.01.006

Mienis, F., De Stigter, H. C., White, M., Duineveld, G., De Haas, H., and Van Weering, T. C. E. (2007). Hydrodynamic controls on cold-water coral growth and carbonate-mound development at the SW and SE rockall trough margin, NE Atlantic ocean. *Deep Sea Res. I* 54, 1655–1674. doi: 10.1016/j.dsr.2007.05.013

Mienis, F., Duineveld, G. C. A., Davies, A. J., Lavaleye, M. M. S., Ross, S. W., Seim, H., et al. (2014). Cold-water coral growth under extreme environmental conditions, the cape lookout area, NW Atlantic. *Biogeosciences* 11, 2543–2560. doi: 10.5194/bg-11-2543-2014

Mienis, F., Duineveld, G. C. A., Davies, A. J., Ross, S. W., Seim, H., Bane, J., et al. (2012). The influence of near-bed hydrodynamic conditions on cold-water corals in the viosca knoll area, gulf of Mexico. *Deep Sea Res. Part I: Oceanogr. Res. Papers* 60, 32–45. doi: 10.1016/j.jmarsys.2012.02.002

Mienis, F., Van Weering, T., De Haas, H., De Stigter, H., Huvenne, V., and Wheeler, A. (2006). Carbonate mound development at the SW rockall trough margin based on high resolution TOBI and seismic recording. *Mar. Geol* 233, 1–19. doi: 10.1016/j.margeo.2006.08.003

Milliman, J. D. (1993). Production and accumulation of calcium carbonate in the ocean: Budget of a nonsteady state. *Global Biogeochemical Cycles* 7, 927–957. doi: 10.1029/93GB02524

Mohn, C., Rengstorf, A., White, M., Duineveld, G., Mienis, F., Soetaert, K., et al. (2014). Linking benthic hydrodynamics and cold-water coral occurrences: A high-resolution model study at three cold-water coral provinces in the NE Atlantic. *Prog. Oceanography* 122, 92–104. doi: 10.1016/j.pocean.2013.12.003

Mohrholz, V., Bartholomae, C. H., van der Plas, A. K., and Lass, H. U. (2008). The seasonal variability of the northern benguela undercurrent and its relation to the oxygen budget on the shelf. *Continental Shelf Res.* 28, 424–441. doi: 10.1016/j.csr.2007.10.001

Mortensen, P. B., Hovland, M., Fosså, J. H., and Furevik, D. M. (2001). Distribution, abundance and size of *Lophelia pertusa* coral reefs in mid-Norway in relation to seabed characteristics. *J. Mar. Biol. Assoc. United Kingdom* 51, 999–1013. doi: 10.1017/S002531540100426X

Mueller, C. E., Larsson, A. I., Veuger, B., Middelburg, J. J., and Van Oevelen, D. (2014). Opportunistic feeding on various organic food sources by the cold-water coral *Lophelia pertusa*. *Biogeosciences* 11, 123–133. doi: 10.5194/bg-11-123-2014

Peura, M., and Iivarinen, J. (1997). "Efficiency of simple shape descriptors" in *Advances in visual form analysis*. Eds. C. A., L. P. Cordella and G. Sanniti Di Baja (Singapore: World Scientific), 443–451.

Pomar, L., Morsilli, M., Hallock, P., and Bádenas, B. (2012). Internal waves, an under-explored source of turbulence events in the sedimentary record. *Earth-Science Rev.* 111, 56–81. doi: 10.1016/j.earscirev.2011.12.005

Price, D. M., Robert, K., Callaway, A., Lo Lacono, C., Hall, R. A., and Huvenne, V. (2019). Using 3D photogrammetry from ROV video to quantify cold-water coral reef structural complexity and investigate its influence on biodiversity and community assemblage. *Coral Reefs* 38, 1007–1021. doi: 10.1007/s00338-019-01827-3

Purkis, S. J., and Harris, P. (2017). Quantitative interrogation of a fossilized carbonate sand body – the pleistocene Miami oolite of south Florida. *Sedimentology* 64, 1439–1464. doi: 10.1111/sed.12367

Purkis, S. J., Koppel, J. V. D., Burgess, P. M., Budd, D. A., Hajek, E. A., and Purkis, S. J. (2016). "Spatial self-organization in carbonate depositional environments," in *Autogenic dynamics and self-organization in sedimentary systems*. Eds. D. A. Budd, E. A. Hajek and S. J. Purkis (Tulsa, Oklahoma: SEPM Society for Sedimentary Geology), 216.

Purkis, S. J., Rowlands, G. P., Riegl, B. M., and Renaud, P. G. (2010). The paradox of tropical karst morphology in the coral reefs of the arid middle East. *Geology* 38, 227–230. doi: 10.1130/G30710.1

Purkis, S. J., Kohler, K. E., Riegl, B. M., and Rohmann, S. O. (2007). The statistics of natural shapes in modern coral reef landscapes. *J. Geol.* 115 (5), 493–508. doi: 10.1086/519774

Raddatz, J., Titschack, J., Frank, N., Freiwald, A., Conforti, A., Osborne, A., et al. (2020). *Solenosmilia variabilis*-bearing cold-water coral mounds off Brazil. *Coral Reefs* 39, 69–83. doi: 10.1007/s00338-019-01882-w

Reed, J. K. (2002). Deep-water *Oculina* coral reefs of Florida: biology, impacts, and management. *Hydrobiologia* 471, 43–55. doi: 10.1023/A:1016588901551

Roberts, J. M., Wheeler, A. J., and Freiwald, A. (2006). Reefs of the deep: The biology and geology of cold-water coral ecosystems. *Science* 312, 543–547. doi: 10.1126/science.1119861

Roberts, J. M., Wheeler, A. J., Freiwald, A., and Cairns, S. D. (2009). *Cold-water corals. the biology and geology of deep-sea coral habitats* (Cambridge, UK: Cambridge University Press).

Savini, A., Vertino, A., Marchese, F., Beuck, L., and Freiwald, A. (2014). Mapping cold-water coral habitats at different scales within the northern Ionian Sea (Central mediterranean): an assessment of coral coverage and associated vulnerability. *PloS One* 9, e87108. doi: 10.1371/journal.pone.0087108

Schlager, W., and Purkis, S. J. (2013). Bucket structure in carbonate accumulations of the maldive, chagos and laccadive archipelagos. *Int. J. Earth Sci.* 102, 2225–2238. doi: 10.1007/s00531-013-0913-5

Schmidt, M., and Eggert, A. (2016). Oxygen cycling in the northern benguela upwelling system: Modellingoxygen sources and sink. *Prog. Oceanogr.* 149, 145–173. doi: 10.1016/j.pocean.2016.09.004

Schroeder, W. W. (2002). Observations of *Lophelia pertusa* and the surficial geology at a deep-water site in the northeastern gulf of Mexico. *Hydrobiologia* 471, 29–33. doi: 10.1023/A:1016580632501

Somoza, L., Ercilla, G., Urgorri, V., León, R., Medialdea, T., Paredes, M., et al. (2014). Detection and mapping of cold-water coral mounds and living *Lophelia* reefs in the Galicia bank, Atlantic NW Iberia margin. *Mar. Geol.* 349, 73–90. doi: 10.1016/j.margeo.2013.12.017

Steinmann, L., Baques, M., Wenau, S., Schwenk, T., Spiess, V., Piola, A. R., et al. (2020). Discovery of a giant cold-water coral mound province along the northern Argentine margin and its link to the regional contourite depositional system and oceanographic setting. *Mar. Geol.* 427, 106223. doi: 10.1016/j.margeo.2020.106223

Tamborrino, L., Wienberg, C., Titschack, J., Wintersteller, P., Mienis, F., Schröder-Ritzrau, A., et al. (2019). Mid-Holocene extinction of cold-water corals on the Namibian shelf steered by the benguela oxygen minimum zone. *Geology* 47, 1185–1188. doi: 10.1130/G46672.1

Taviani, M., Remia, A., Corselli, C., Freiwald, A., Malinverno, E., Mastrototaro, F., et al. (2005). First geo-marine survey of living cold-water *Lophelia* reefs in the Ionian Sea (Mediterranean basin). *Facies* 50, 409–417. doi: 10.1007/s10347-004-0039-0

Thiem, Ø., Ravagnan, E., Fosså, J. H., and Berntsen, J. (2006). Food supply mechanisms for cold-water corals along a continental shelf edge. *J. Mar. Syst.* 60, 207–219. doi: 10.1016/j.jmarsys.2005.12.004

Titschack, J., Baum, D., De Pol Holz, R., López Correa, M., Forster, N., Flögel, S., et al. (2015). Aggradation and carbonate accumulation of Holocene Norwegian cold-water coral reefs. *Sedimentology* 62, 1873–1898. doi: 10.1111/sed.12206

Titschack, J., Fink, H. G., Baum, D., Wienberg, C., Hebbeln, D., and Freiwald, A. (2016). Mediterranean Cold-water corals – an important regional carbonate factory? *Depositional Rec.* 2, 74–96. doi: 10.1002/dep2.14

Titschack, J., Thierens, M., Dorschel, B., Schulbert, C., Freiwald, A., Kano, A., et al. (2009). Carbonate budget of a cold-water coral mound (Challenger mound, IODP exp. 307). *Mar. Geology* 259, 36–46. doi: 10.1016/j.margeo.2008.12.007

Vandorpe, T., Wienberg, C., Hebbeln, D., Van Den Berghe, M., Gaide, S., Wintersteller, P., et al. (2017). Multiple generations of buried cold-water coral mounds since the early-middle pleistocene transition in the Atlantic Moroccan coral province, southern gulf of cádiz. *Palaeogeography Palaeoclimatology Palaeoecol.* 485, 293–304. doi: 10.1016/j.palaeo.2017.06.021

van Haren, H., and Gostiaux, L. (2012). Energy release through internal wave breaking. *Oceanography* 25, 124–131. doi: 10.5670/oceanog.2012.47

van Haren, H., Mienis, F., Duineveld, G. C. A., and Lavaleye, M. S. S. (2014). High-resolution temperature observations of a trapped nonlinear diurnal tide influencing cold-water corals on the logachev mounds. *Prog. Oceanography* 125, 16–25. doi: 10.1016/j.pocean.2014.04.021

Van Rooij, D., De Mol, B., Huvenne, V., Ivanov, M., and Henriet, J. P. (2003). Seismic evidence of current-controlled sedimentation in the Belgica mound province, upper Porcupine slope, southwest of Ireland. *Mar. Geol.* 195 (1-4), 31–53. doi: 10.1016/S0025-3227(02)00681-3

von Bodungen, B., John, E.-C., Lutjeharms, J. R. E., Mohrholz, V., and Veitch, J. (2008). Hydrographic and biological patterns across the Angola–benguela frontal zone under undisturbed conditions. *J. Mar. Syst.* 74, 189–215. doi: 10.1016/j.jmarsys.2007.12.007

Wang, B., Bogucki, D., and Redekopp, L. (2001). Internal solitary waves in a structured thermocline with implications for resuspension and the formation of thin particle-laden layers. *J. Geophysical Research: Oceans* 106, 9565–9585. doi: 10.1029/2000JC900101

Wang, H., Lo Iacono, C., Wienberg, C., Titschack, J., and Hebbeln, D. (2019). Cold-water coral mounds in the southern alboran Sea (western Mediterranean sea): Internal waves as an important driver for mound formation since the last deglaciation. *Mar. Geology* 412, 1–18. doi: 10.1016/j.margeo.2019.02.007

Wang, H., Titschack, J., Wienberg, C., Korpanty, C., and Hebbeln, D. (2021). The importance of ecological accommodation space and sediment supply for cold-water coral mound formation, a case study from the Western Mediterranean Sea. *Front. Mar. Sci.* 8. doi: 10.3389/fmars.2021.760909

Westphal, H., Beuck, L., Braun, S., Freiwald, A., Hanebuth, T., Hetzinger, S., et al. (2012). "Phaeton. cruise report of cruise no. MSM16/3, 13.10.-20.11 2010, bremerhaven-mindelo," in *MARIA s. MERIAN-berichte* (Bremen, Germany: Institut für Meereskunde, Univ Hamburg).

Wheeler, A. J., Beyer, A., Freiwald, A., De Haas, H., Huvenne, V., Kozachenko, M., et al. (2007). Morphology and environment of cold-water coral carbonate mounds on the NW European margin. *Int. J. Earth Sci.* 96, 37–56. doi: 10.1007/s00531-006-0130-6

Wheeler, A. J., Kozachenko, M., Henry, L. A., Foubert, A., De Haas, H., Huvenne, V., et al. (2011). The moira mounds, small cold-water coral banks in the porcupine seabight, NE Atlantic: Part a–an early stage growth phase for future coral carbonate mounds? *Mar. Geology* 282, 53–64. doi: 10.1016/j.margeo.2010.08.006

Wheeler, A. J., Kozachenko, M., Masson, D. G., and Huvenne, V. (2008). Influence of benthic sediment transport on cold-water coral bank morphology and growth: the example of the Darwin mounds, north-east Atlantic. *Sedimentology* 55, 1875–1887. doi: 10.1111/j.1365-3091.2008.00970.x

White, M. (2003). Comparison of near seabed currents at two locations in the porcupine Sea bight–implications for benthic fauna. *J. Mar. Biol. Assoc. United Kingdom* 83, 683–686. doi: 10.1017/S0025315403007641h

White, M., and Dorschel, B. (2010). The importance of the permanent thermocline to the cold water coral carbonate mound distribution in the NE Atlantic. *Earth Planetary Sci. Lett.* 296, 395–402. doi: 10.1016/j.epsl.2010.05.025

White, M., Mohn, C., De Stigter, H., and Mottram, G. (2005). ""Deep-water coral development as a function of hydrodynamics and surface productivity around the submarine banks of the rockall trough, NE atlantic,"," in *Cold-water corals and ecosystems*. Eds. A. Freiwald and J. M. Roberts (Heidelberg: Springer), 503–514.

Wienberg, C., Beuck, L., Heidkamp, S., Hebbeln, D., Freiwald, A., Pfannkuche, O., et al. (2008). Franken mound: facies and biocoenoses on a newly-discovered "carbonate mound" on the western rockall bank, NE Atlantic. *Facies* 54, 1–24. doi: 10.1007/s10347-007-0118-0

Wienberg, C., Hebbeln, D., Fink, H. G., Mienis, F., Dorschel, B., Vertino, A., et al. (2009). Scleractinian cold-water corals in the gulf of cadiz-first clues about their spatial and temporal distribution. *Deep-Sea Res. Part I-Oceanographic Res. Papers* 56, 1873–1893. doi: 10.1016/j.dsr.2009.05.016

Wienberg, C., and Titschack, J. (2017). "Framework-forming scleractinian cold-water corals through space and time: A late quaternary north Atlantic perspective," in *Marine animal forests: The ecology of benthic biodiversity hotspots*. Eds. S. Rossi, L. Bramanti, A. Gori and C. Orejas Saco Del Valle (Cham: Springer), 699–732.

Wienberg, C., Titschack, J., Frank, N., De Pol-Holz, R., Fietzke, J., Eisele, M., et al. (2020). Deglacial upslope shift of NE Atlantic intermediate waters controlled slope erosion and cold-water coral mound formation (Porcupine seabight, Irish margin). *Quaternary Sci. Rev.* 237, 106310. doi: 10.1016/j.quascirev.2020.106310

Wilson, J. B. (1979). "Patch" development of the deep-water coral *Lophelia pertusa* (L.) on the rockall bank. *J. Mar. Biol. Assoc. United Kingdom* 59, 165–177. doi: 10.1017/S0025315400046257

Zabel, M., Mohrholz, V., Schulz-Vogt, H., Sommer, S., and Zettler, M. (2019). "The benguela system under climate change effects of variability in physical forcing on carbon and oxygen budgets." *Cruise M157, 04.08.2019 - 16.09.2019, mindelo (Cape Verde) - Walvis bay (Namibia). METEOR-Berichte/Reports, M157DFG-senatskommission für ozeanographie* (Bremen; METEOR-Berichte), 58.